



Naturalis Repository

## Beydere 3: a new early Miocene small mammal assemblage from western Anatolia, Turkey

Melike Bilgin, Peter Joniak, Pablo Peláez Campomanes, Fikret Göktaş, Serdar Mayda, Coen Lorinser, Jan Wijbrans, Tanju Kaya and Lars W. van den Hoek Ostende

DOI:

<https://doi.org/10.1080/08912963.2022.2077646>

Downloaded from

[Naturalis Repository](#)

### Article 25fa Dutch Copyright Act (DCA) - End User Rights

This publication is distributed under the terms of Article 25fa of the Dutch Copyright Act (Auteurswet) with consent from the author. Dutch law entitles the maker of a short scientific work funded either wholly or partially by Dutch public funds to make that work publicly available following a reasonable period after the work was first published, provided that reference is made to the source of the first publication of the work.

This publication is distributed under the Naturalis Biodiversity Center 'Taverne implementation' programme. In this programme, research output of Naturalis researchers and collection managers that complies with the legal requirements of Article 25fa of the Dutch Copyright Act is distributed online and free of barriers in the Naturalis institutional repository. Research output is distributed six months after its first online publication in the original published version and with proper attribution to the source of the original publication.

You are permitted to download and use the publication for personal purposes. All rights remain with the author(s) and copyrights owner(s) of this work. Any use of the publication other than authorized under this license or copyright law is prohibited.

If you believe that digital publication of certain material infringes any of your rights or (privacy) interests, please let the department of Collection Information know, stating your reasons. In case of a legitimate complaint, Collection Information will make the material inaccessible. Please contact us through email: [collectie.informatie@naturalis.nl](mailto:collectie.informatie@naturalis.nl). We will contact you as soon as possible.



## Beydere 3: a new early Miocene small mammal assemblage from western Anatolia, Turkey

Melike Bilgin<sup>a,b</sup>, Peter Joniak<sup>a</sup>, Pablo Peláez Campomanes<sup>c</sup>, Fikret Göktaş<sup>d</sup>, Serdar Mayda<sup>e</sup>, Coen Lorinser<sup>f</sup>, Jan Wijbrans<sup>g</sup>, Tanju Kaya<sup>e</sup> and Lars W. van den Hoek Ostende<sup>b</sup>

<sup>a</sup>Department of Geology and Palaeontology, Comenius University, Bratislava, Slovakia; <sup>b</sup>Naturalis Biodiversity Center, Leiden, The Netherlands; <sup>c</sup>Museo Nacional de Ciencias Naturales - CSIC, Madrid, Spain; <sup>d</sup>MTA Geology Department, Ankara, Turkey; <sup>e</sup>Faculty of Science, Biology Department, Ege University, Izmir, Turkey; <sup>f</sup>Instituut Biologie Leiden, Universiteit Leiden, Leiden, Netherlands; <sup>g</sup>Department of Earth Sciences, Cluster Geology and Geochemistry, Vrije Universiteit Amsterdam, Amsterdam, The Netherlands

### ABSTRACT

The new micromammal site of Beydere 3 represents a typical Anatolian MN3 fauna in the high diversification and abundance of *Eumyarion*. Notably, two *Eumyarion* species are new; combined, they make up almost half of the assemblage. While *Eumyarion beyderensis* sp. nov. shows simple morphology in upper molars, *Eumyarion aegeaniensis* sp. nov. shows a more complex loph pattern. In addition, Beydere 3 yielded nine species of rodents and an ochotonid: the hamsters *Cricetodon kasapligili*, *Mirabella crenulata*, *Megacricetodon hellenicus*, *Democricetodon doukasi*, *Vallaris zappai* and *Eumyarion* sp., the dormice *Glirulus ekremi* and *Glis* sp., the beaver *Steneofiber eseri*, the squirrel *Palaeosciurus fissurae* and Ochotonidae indet. The fauna is significant in that it represents the first common occurrence of *Megacricetodon* in Anatolia. *Eumyarion* and *Megacricetodon* are both dominant groups which may indicate a signal of environmental change, but still closer to wet conditions. This, in combination with the new species of *Eumyarion*, suggests that Beydere 3 represents a time slice which was previously not recorded in Anatolia. Radiometric dating of ashes overlying the section indicates that the age of the locality is older than 18.21 (± 0.19) Ma.

### ARTICLE HISTORY

Received 18 February 2022  
Accepted 11 May 2022

### KEYWORDS

Rodentia; Lagomorpha;  
biostratigraphy; taxonomy

### Introduction

The early Miocene rodent fauna of Anatolia has been extensively studied since the 1990's. Localities such as Kılçak, Harami, Gökler, Gördes, Sabuncubeli, Bornova, Keseköy and Çapak have had their small mammal assemblages described and combined provide a picture of distribution and migration patterns during the early Miocene (De Bruijn and Saraç 1991, 1992; Van den Hoek Ostende 1992; De Bruijn and von Koenigswald 1994; Ünay 1994, 1995a, 1995b, 1997, 2001, 2006; Joniak et al. 2017; Bilgin et al. 2019, 2019; Peláez-Campomanes et al. 2019, 2021). Apart from these extensively studied localities, there are many localities that are known only from fauna lists. The early Miocene deposits near the village of Beydere (Manisa, Turkey) have been known by scientists since the 2000s. Preliminary palaeontological research in the area has been done by Saraç (2003) and Kaya et al. (2007). The report of Saraç (2003) refers to two localities in the Bozalan district: Beydere 1 and Beydere 2, while Kaya et al. (2007) do not mention the locality name but indicate two fossiliferous layers in the Bozalan area from the middle and uppermost part of the Soma Formation, respectively (in Kaya et al. 2007, p. 91 and p. 94). The combined records from Saraç (2003) and Kaya et al. (2007) suggest that Beydere 1 represents the layer in the middle part of the formation, whereas Beydere 2 and the one from the uppermost part of the formation are probably the same locality. However, the faunal lists of two studies differ, presumably because of new identifications. Based on the faunal content, Saraç (2003) and Kaya et al. (2007) correlated these localities to MN4. According to Kaya et al. (2007), the fauna from the middle part of the formation contains *Cricetodon* sp.,

*Eumyarion* sp., *Galerix* sp., *Glirulus* sp., *Megacricetodon* sp., *Tamias* sp. and Lagomorpha indet. The uppermost part of the formation contains *Cricetodon* sp., *Eumyarion* sp., *Democricetodon* sp., *Glirudinus* sp. and Castoridae indet.

Here, we present another fossiliferous layer from the same area in the Soma Formation. The locality of Beydere 3 was found in the scope of the National Geographic project “Palaeogeography of Anatolian mammals following the collision of the African and Eurasian plates” in 2015. Beydere 3 is located one kilometre east of Beydere 1 near the Beydere village in the north-west part of the Manisa Province (Figure 1a). The assemblage represents a time interval that is not well known from Anatolia and provides important data for interpretation of the development of micromammal assemblages within the eastern Mediterranean. In this paper, we describe the rodents and the lagomorph from this locality. The Eulipotyphla assemblage will be published elsewhere.


### Material and methods

Around 1500 kg of sediment was collected in 2015 and 2018 field-work campaigns. The sediment was screen-washed with a mesh of 0.5 mm following the method of Daams and Freudenthal (1988a). The concentrate was reduced with acetic acid before it was sorted under the microscope. As a result, 306 small mammal molars were obtained.

Upper cheek teeth are indicated by uppercase and lower cheek teeth by lowercase. Where distinction between first and second molars is questionable, these are indicated as m1/2 or M1/2,

**CONTACT** Melike Bilgin  [bilgin1@uniba.sk](mailto:bilgin1@uniba.sk)  Department of Geology and Palaeontology, Comenius University, Bratislava, Slovakia

UUID: <http://zoobank.org/81906ECD-421B-44B4-A6E0-605683003CEB><http://zoobank.org/F2C9A449-DA65-4262-A221-624F0FD00C2F>

 Supplemental data for this article can be accessed online at <https://doi.org/10.1080/08912963.2022.2077646>

© 2022 Informa UK Limited, trading as Taylor & Francis Group



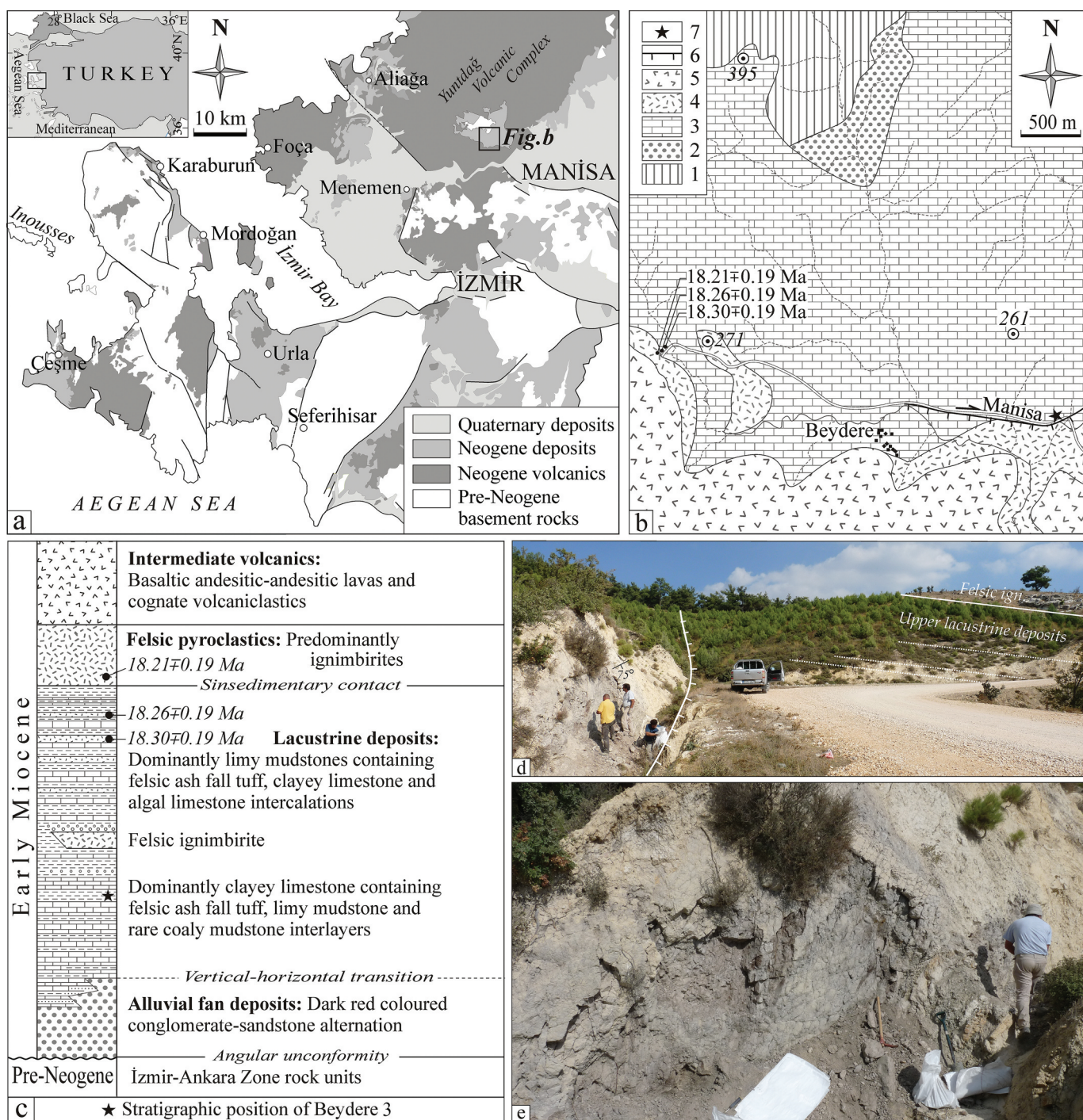


**Figure 1.** Geographical and stratigraphical position of Beydere 3 locality. **a)** Geological setting of study area **b)** Simplified geological map of the study area: 1 Pre-Neogene Izmir-Ankara Zone rocks, 2 Lower Miocene alluvial fan deposits, 3 Lower Miocene lacustrine deposits, 4 Mainly felsic ignimbrites, 5 Intermediate volcanics, 6 Normal fault, 7 Beydere 3 locality **c)** Generalised stratigraphic succession of the study area. **d)** Outcrop view of Beydere 3 locality **e)** The fossiliferous layer of Beydere 3.

respectively. Tooth measurements (maximum length and width) are given in mm and were taken using a digital measuring microscope with mechanical stage and digital measuring clocks. The terminology used for teeth parts follows Daams and Freudenthal (1988b) and Oliver and Peláez-Campomanes (2013) for Muridae, García-Paredes et al. (2010) for Gliridae, Cuenca-Bescós (1988) for Sciuridae, Huguency (1999) for Castoridae and López Martínez (1986) for Ochotonidae. The SEM photographs were taken at the Slovak Academy of Sciences. All dental elements have been figured as being left; the letters of mirrored photographs

have been underlined on the plates. The material is stored in the collections of the Natural History Museum of the Ege University in Izmir, Turkey.

#### **<sup>40</sup>Ar/<sup>39</sup>Ar analytical procedure and results**

Basalt samples were crushed and sieved. The 250–500 micrometre fraction was selected for further treatment. In order to remove phenocryst fractions and altered material, the sieved fractions density separation was carried out with organic heavy liquids (CH<sub>2</sub>I<sub>2</sub>)

adjusted to the density of 2.65 g/cm<sup>3</sup> and 2.90 g/cm<sup>3</sup>. The samples were wrapped in Al-foil and loaded in 20 mm OD Al capsules. Sample packages and ca. 5 mg aliquots of laboratory standard sanidine DRA-2 (25.42 Ma), intercalibrated against FC sanidine at 28.20 Ma (Wijbrans et al. 1995), recalculated to Kuiper et al. 2008) were wrapped in Cu-foil and loaded on top and bottom positions in the quartz vial and between each of 3–5 samples. Samples were irradiated in the Oregon State University TRIGA reactor in the cadmium shielded CLICIT facility for 7 hours. After irradiation, the samples and standards were loaded at VU Amsterdam in a copper sample tray (diameter 66 mm, sample holes 2 mm diameter, 3 mm depth, 185 positions, for the standards, and 21 holes 6 mm wide for the unknowns) and placed in an ultrahigh vacuum extraction line. The standards were directly fused and analysed isotopically with a Hiden triple filter quadrupole mass spectrometer (Schneider et al. 2009). In a second step, selected samples were introduced in a copper sample tray with 66 mm diameter and 21 sample holes of 6 mm diameter and 3 mm depth and were measured by stepwise heating in 22–25 laser intensity steps using a continuous wave 25 W CO<sub>2</sub> laser and a beam delivery line including a 3x beam expander, an iron mesh beam attenuation filter, and an optical scanhead for beam delivery. The scanhead was used for diffusing the laser beam by applying a triangular current with a frequency of 100 Hz, causing a beam width of 2 mm on the X-axis mirror of the scanhead, and superposed on that X-Y rastering to cover all the sample at the bottom of the 6 mm depression in the sample copper tray. Beam intensities of the five isotopes of argon (m/e: 40–36) were measured sequentially by high frequency field controlled peak-jumping mode at half-past intervals over the 40–35.5 mass range with multiple readings taken on the m/e 36, 39 and 40 beams as to improve the counting statistics of the measurements. Beam intensities were measured on a pulse-counting secondary electron multiplier of the channeltron type. System blanks were measured in between each three steps. For data reduction we used the ArArCalc2.5 software package (Koppers 2002) (<http://earthref.org/tools/ararcalc/>). The average value of blank analyses before and after the measurement of an unknown is applied as blank correction for all isotopes. The analytical data are reported as weighted mean <sup>40</sup>Ar/<sup>39</sup>Ar ratios with standard errors of the mean weighted with the inverse of the variance (Taylor 1997). Ages and uncertainties have been calculated according to standard age equations using the consensus decay constants of (Steiger and Jäger 1977). Uncertainties are reported at three levels: (1) analytical uncertainty in the sample and the standard; (2) uncertainty in the absolute age of the standard; and (3) uncertainty in the decay constants as reported in (Steiger and Jäger 1977). All errors are quoted at the 1σ significance level.

#### 40Ar/39Ar results

High resolution 40Ar/39Ar laser incremental heating experiments were performed on three samples from different localities in the Beydere section. Almost all experiments showed good consistent results within some scatter in excess of the accepted values for plateau ages observed. Mean Square Weighted Deviate (MSWD) values were used to assess the scatter (Koppers 2002). All samples showed very high amounts of radiogenic 40Ar and high K/Ca ratios pointing to a potassium enriched volcanic source. Most of the samples show elevated ages in the initial steps which may either correspond to loosely bound excess 40Ar or, alternatively, to recoil loss of 39Ar (Koppers 2002). Excess scatter points may be due to mild alteration of the material used for dating. However, despite this observed mild scatter, an early Miocene age for all three samples is undisputed.

From the 39Ar and 37Ar amounts released during the experiments we can gain some information on the chemical composition of the analysed mineral phases contributing to the spectrum in terms of their potassium and calcium contents, where 37Ar is a proxy for calcium and 39Ar is a proxy for potassium. The K/Ca plots show that in the lower temperature steps the gas is derived dominantly from K-rich mineral parts, whereas at higher experimental temperatures the Ca-rich phases predominate (Wijbrans et al. 2007), albeit with substantial scatter. Due to the high enrichment in radiogenic argon, points plotted in a cluster very near to the horizontal axis in the inverse isochron plot. In such cases, we tend to report the age recorded in the age spectrum as representing the best estimate of the depositional age.

The tuff levels located in the upper parts of the succession are dated at 18.26 ± 0.19 Ma and 18.30 ± 0.19 Ma based on 40Ar/39Ar dating. Felsic (rhyolitic?) pyroclastics overlie the lacustrine succession synsedimentary unit (Figure 1). The pyroclastic sequence consists predominantly of whitish light grey coloured ignimbrites. Pumice in the first ignimbrite level overlying lacustrine deposits is dated at 18.21 ± 0.19 Ma based on 40Ar/39Ar dating.

All the data tables are in the supplement documents.

#### Geology

The small mammal fauna of Beydere 3 has been found 20 km NE of Manisa (38.682955, 27.264251), within an erosional window covered by the Yundağ vulcanite onto the lacustrine deposit (Akyürek and Soysal 1981) (Figure 1a). Lacustrine sedimentation starts with alluvial fan deposits and ends with the settlement of felsic ignimbrites in the basin, which is overlying on the 'İzmir-Ankara Zone' (Brinkmann 1966) rocks with angular unconformity (Figure 1b,c). The alluvial fan succession is represented by a dark red conglomerate-sandstone alternation. The lacustrine succession, which overlies alluvial deposits with a lateral-vertical transition, consists of limestone-mudstone alternation, the relative lithological composition of which changes from bottom to top. The lower part of the lacustrine succession is dominated by limestones, while mudstones are found in the upper part. Limestones that have a yellowish weathering surface generally have regular medium-bedding. The limestone dominant succession forming the lower section includes massive mudstone and felsic ashfall tuff interfaces with thicknesses ranging from centimetres to decimetres. Mudstones with varying proportions of calcareous are green, while blackish/dark brown at the levels with higher organic matter content and light grey at the tuff levels. The Beydere 3 fauna was found in one of the calcareous mudstone levels containing dense gastropod shell fragments and tuffogenes (Figure 1d,e). The mudstone-dominated succession forming the upper part consists of metres thick mudstones that contain tuffogenes. There are clayey limestone, algal-oncoidal limestone and felsic ashfall tuff interfaces in the massive mudstones with variable organic matter content and lime content.

#### Systematic palaeontology

Order Rodentia Bowdich 1821

Family Muridae Illiger 1811

Genus *Cricetodon* Lartet 1851

*Cricetodon kasapligili* De Bruijn, Fahlbusch, Saraç and Ünay 1993  
Figure 2 A–C

**Material and measurement:** 1 M2 (PV13360, 1.85 × 1.70), 2 M3 (PV13362, 1.81 × 1.71; PV13363, 1.72 × 1.66), 1 m1 (PV13361, 2.39 × 1.58)



### Description

**M2.** The lingual anteroloph is short and descends to the base of the protocone. The labial anteroloph is well developed and connects to the base of the paracone. The protolophule and the metalophule are single and parallel, directed posteriorly. The metalophule is almost connected to the posteroloph. The posterior paracone spur is weak. The mesoloph is medium length. The posteroloph is connected to the metacone enclosing the posterosinus. The sinus is directed slightly anteriorly. The roots are not preserved.

**M3.** The lingual anteroloph descends to the base of the protocone and creates a small protosinus. The labial anteroloph is long and connected to the base of the paracone. The protolophule is directed anteriorly in one and directed posteriorly in the other specimen. The posterior paracone spur is absent. The mesoloph is long and it is connected to the labial border in one specimen. The metalophule is connected to the anterior arm of the hypocone. The posteroloph is weak and connected to the posterior arm of the hypocone. The metacone is incorporated with the posteroloph. The sinus is directed anteriorly. The roots are not preserved.

**m1.** The rounded anteroconid is situated on the longitudinal axis of the occlusal surface. The labial and the lingual anterolophids slope down and are not connected to the metaconid and the protoconid, respectively. The metalophulid I is very weak, connected to the anteroconid. The metalophulid II is connected to the posterior arm of the protoconid. The hypolophulid is directed anteriorly and connected to the ectolophid. The mesolophid is very short. The ectomesolophid is much longer than the mesolophid. The posterolophid is well developed and connects to the base of the entoconid. The posterior sulcus and the weak labial posterolophid are present. The roots are not preserved.

### Remarks

*Cricetodon kasapligili* is known from its type locality Keseköy (De Bruijn et al. 1993), from Yapıntı (Durgut and Engin 2016), from Sabuncubeli and Bornova (Bilgin et al. 2019); finds classified as

*Cricetodon cf. kasapligili* were described from Harta (Durgut and Engin 2016) and Gökler (Joniak et al. 2017). The species is distinguished from the other species of this genus from the early Miocene of Anatolia by its simple morphology and larger size. On the other hand, it has a similar morphology but slightly smaller size than *Cricetodon tobieni* from Horlak (De Bruijn et al. 1993). The important difference between these two species lies in the number of the roots in the M1. While *C. kasapligili* has three roots, *C. tobieni* has four. *Cricetodon kasapligili* was originally described from a very small assemblage (eight molars) from Keseköy. Therefore, the variation of the species cannot be assessed from the type locality. For instance, the Beydere 3 specimens are all larger than those from Keseköy, but they fall within the range of *C. kasapligili* from Yapıntı. The M3 is not represented from type locality of Keseköy, but the M3 from Beydere 3 is metrically and morphologically within the variation of Yapıntı specimens (Çınar 2011). The only m1 from Keseköy has, in contrast to the Beydere 3 specimen, a single metalophulid. However, a double metalophulid is found in some of the m1 from Sabuncubeli and Yapıntı. The M2 from Beydere 3 is morphologically similar to the Keseköy specimens. Overall, we do not see any contradiction to attribute these specimens to *Cricetodon kasapligili*.

Genus *Mirrabella* De Bruijn, Van den Hoek Ostende and Donovan 2007

*Mirrabella crenulata* (De Bruijn, Saraç, Jost and Ünay 1992)

### Figure 2 D–G

**Material and measurements:** 1 M2 (PV13350,  $2.12 \times 1.74$ ), 2 M3 (PV13351,  $1.50 \times 1.57$ ; PV13358,  $\sim 1.72 \times 1.51$ ), 3 m1 (PV13352,  $2.62 \times 1.54$ ; PV13353,  $2.65 \times 1.51$ ; PV13354, – x –), 3 m3 (PV13355, – x –; PV13356,  $2.19 \times 1.51$ ; PV13357, – x –)

### Description

**M2.** The labial anteroloph is longer and better developed than the lingual anteroloph. The protolophule I is short and connects to the middle part of the labial anteroloph. The protolophule II is long,

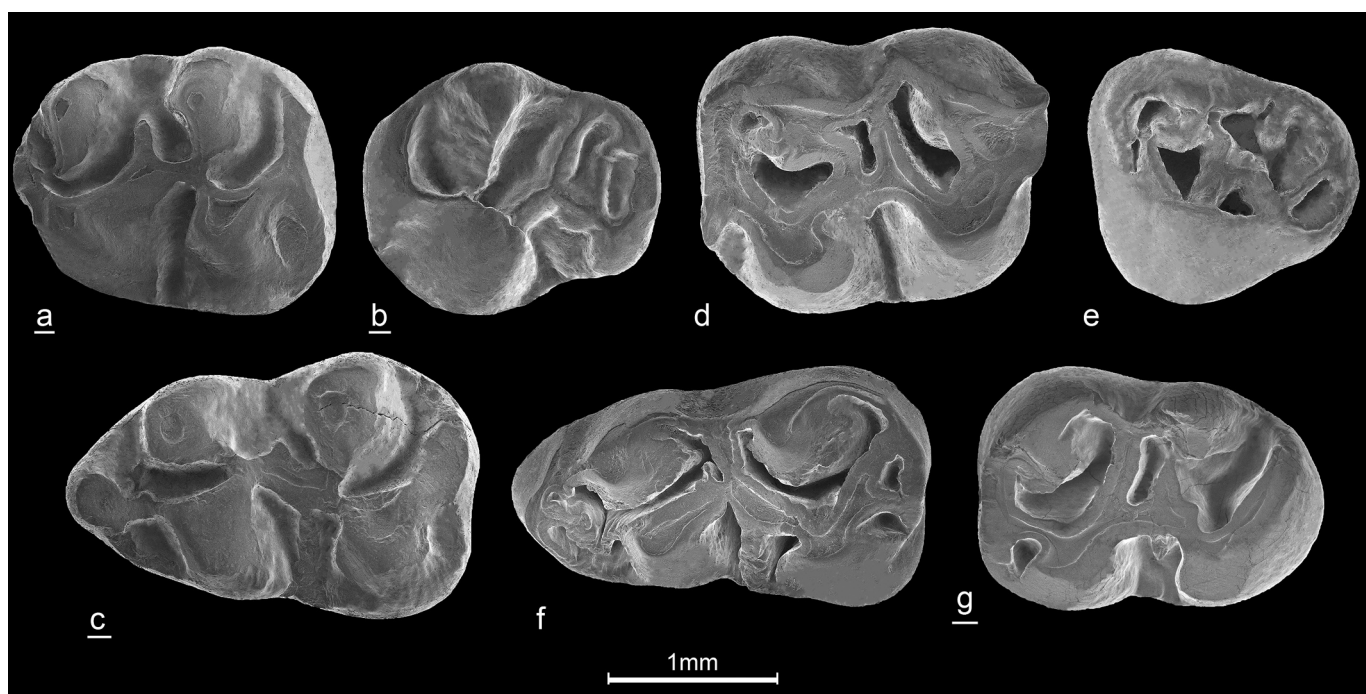


**Figure 2.** *Cricetodon kasapligili* (A) M2 dex (PV13360), (B) M3 dex (PV13362), (C) m1 dex (PV13361); *Mirrabella crenulata* (D) M2 sin (PV13350), (E) M3 sin (PV13351), (F) m1 sin (PV13352), (G) m3 dex (PV13356).

oblique and connects to the posterior arm of the protocone. The posterior paracone spur and the anterior arm of the metacone are strong and connect to the long mesoloph. The metalophule is single and connects to the hypocone. The posteroloph is very short and is fused with the strong posterior spur of the metacone. The sinus is deep. The roots are not preserved.

**M3.** The molars are slightly elongated. The lingual anteroloph is absent. The labial anteroloph is connected to the paracone. The protolophule I is irregular, but generally directed anteriorly and connected to the anterior part of the protocone. The protolophule II is also irregular and connects to the protocone centrally. The posterior paracone spur is connected to the metacone and forms the labial wall of the tooth. The metacone is incorporated with the posteroloph. The metalophule is single, connected to the mure and interrupted by the mesoloph. The sinus is closed. The roots are not preserved.

**m1.** The anterior part of the molar is triangular in occlusal view. The lingual anterolophid is connected to the metaconid. The labial anterolophid is connected to the base of the protoconid. The posterior arm of the protoconid, the anterior arm of the hypoconid and strong mesolophid are connected in the centre of the molar. The mesolophid ends in the lingual crest of the molar. The sinusid is wide and divided by the strong ectomesolophid. The ectomesolophid and the mesolophid are not in one line. The hypolophulid is absent. The posterior arm of the hypoconid is very strong and connects to the posterolophid in two places in one specimen, while this double connection is not visible in the other specimen because of the stage of the wear. The roots are not preserved.

**m3.** The lingual anterolophid is longer than the labial one and connects to the metaconid. The metalophulid is absent. The posterior arm of the protoconid is long and reaches to the lingual edge. The mesolophid is of medium length. The ectomesolophid is present in one and absent in two specimens. The lingual side of the posterolophid is low and the posterosinusid is open. The sinusid is wide. The molar has two roots.

### Remarks

The genus *Mirrabella* is known from the several early Miocene Anatolian assemblages, from Bosnia and Herzegovina and from Greece. A single molar (*Mirrabella* sp.) is recorded from German locality Rembach, as well (Prieto and Rummel 2016). The species are from the most primitive: *Mirrabella* aff. *anatolica* from Banovići, *M. anatolica* from Harami 1, *M. anatolica/crenulata* exemplum intercentrale from Sabuncubeli, *M. crenulata* from Keseköy and *M. tuberosa* from Aliveri (e.g., De Bruijn and Saraç 1992, 2006, 2013; Joniak et al. 2019). Beydere 3 specimens are metrically comparable with *M. anatolica*, *M. anatolica/crenulata* exemplum intercentrale and *M. crenulata*. Morphologically, it is similar to *M. crenulata*, from its type locality of Keseköy. There is only a difference in the morphology of the m1. The m1 from Beydere 3 has a longer anterior arm of the hypoconid which continues into the lingual crest; the posterior arm of the protoconid connects to the anterior arm of the hypoconid in the centre of the loph. However, the m1 from Keseköy has a connection between the anterior arm of the hypoconid and posterior arm of the protoconid in the centre of the molar. Since all the other features are the same as in the type assemblage, we attribute *Mirrabella* from Beydere 3 to *M. crenulata*.

Genus *Eumyarion* Thaler 1966

*Eumyarion beyderensis* sp. nov.

### Figure 3

**Derivatio nominis.** After the type locality Beydere 3 in western Anatolia, Turkey.

**Holotype.** Left M1(PV13538, 2.06 × 1.47), **Figure 3B**

**Type locality.** Beydere 3 (Manisa/Turkey)

**Age.** early Miocene, local zone D (MN3)

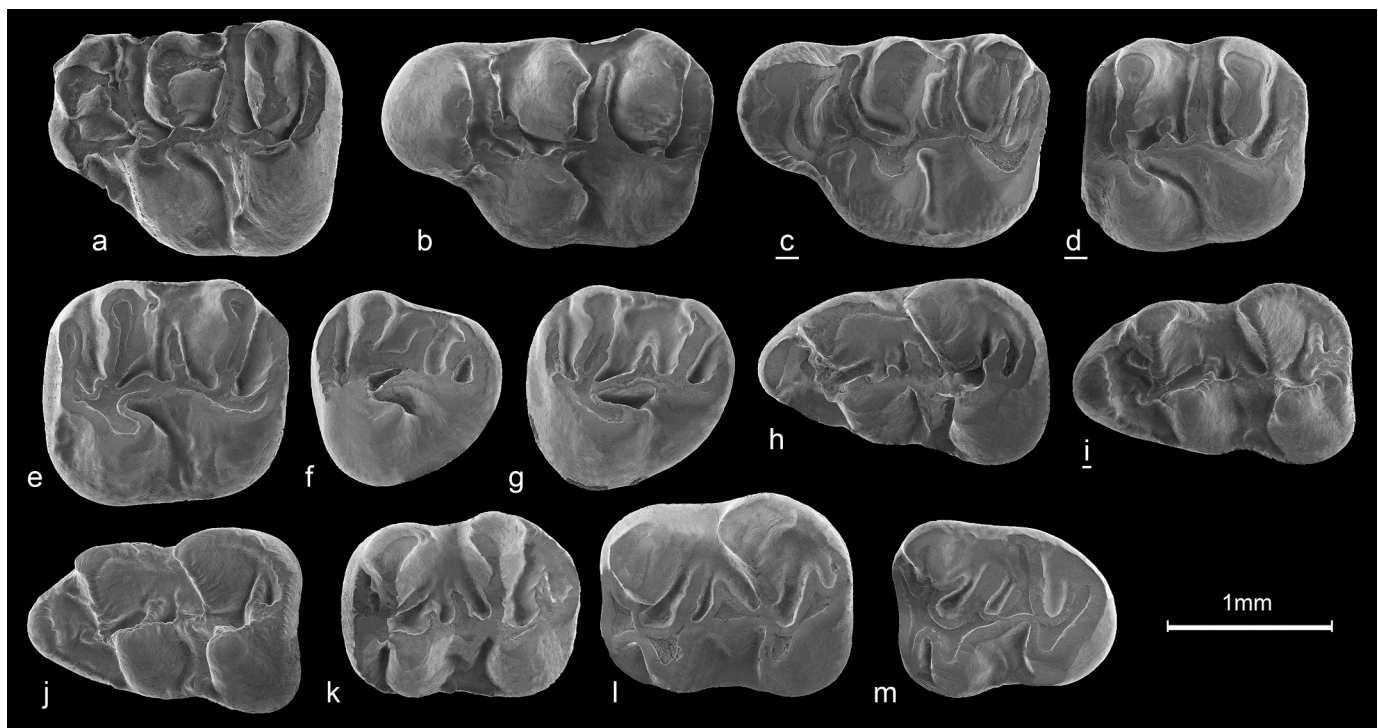


**Figure 3.** *Eumyarion beyderensis* sp. nov. (A) M1 sin (PV13537), (B) M1 sin (PV13538), (C) M1 dex (PV13541), (D) M2 dex (PV13546), (E) M2 sin (PV13542), (F) M3 sin (PV13549), (G) M3 sin (PV13548), (H) m1 sin (PV13575), (I) m1 dex (PV13596), (J) m1 sin (PV13561), (K) m2 sin (PV13578), (L) m2 dex (PV13577), (M) m3 sin (PV13565).

**Material.** 4 M1 (PV13537 – PV13540), 8 M2 (PV13525, PV13526, PV13542 – 13,546, PV13574), 5 M3 (PV13548 – PV13552), 9 m1 (PV13553, PV13554, PV13556 – PV13561, PV13575), 2 m2 (PV13577, PV13578), 1 m3 (PV13565)

**Measurements.** Measurements of cheek teeth are given in Table 1.

**Table 1.** Measurements of *Eumyarion beyderensis* sp. nov.

	Length				N	Width			
	min	mean	max	SD		min	mean	max	SD
M1	1.96	2.02	2.06	0.037	4/4	1.33	1.41	1.47	0.059
M2	1.40	1.50	1.57	0.044	9/9	1.31	1.43	1.48	0.036
M3	1.22	1.25	1.30	0.027	5/5	1.16	1.24	1.32	0.054
m1	1.75	1.81	1.90	0.049	9/9	1.14	1.19	1.23	0.025
m2	1.51	-	1.61	-	2/2	1.17	-	1.33	-
m3	-	1.46	-	-	1/1	-	1.22	-	-

**Diagnosis.** *Eumyarion* of medium size. Upper and lower molars with inflated cusps and thick crests. M1 and M2 with a small posterior paracone spur. M1 with a large anterocone, well-developed anterior arm of the protocone and with a long mesoloph. M2 with a free-ending labial anteroloph and with a single protolophule. Lower m1 and m2 with a well-developed posterior arm of the hypoconid and medium to short mesolophid that is not connected to the posterior arm of the protoconid.

**Differential diagnosis.** *Eumyarion beyderensis* differs from *E. microps* De Bruijn and Saraç 1991, *E. intercentralis* De Bruijn and Saraç 1991, *E. orhani* De Bruijn et al. 2006, *E. leemanni* (Hartenberger 1965), *E. gordesensis* Peláez Campomanes et al. 2019, *E. carbonicus* De Bruijn and Saraç 1991, and *E. weinfurteri* (Schaub and Zapfe 1953) by its larger size.

*Eumyarion beyderensis* differs from *E. margueritae* De Bruijn et al. 2013, *E. montanus* De Bruijn and Saraç 1991 and *E. medius* (Lartet 1851) by its smaller size. It overlaps in size with *E. lukasi* Joniak et al. 2017, *E. bifidus* (Fahlbusch 1964) and with the larger specimens of *Eumyarion aegeaniensis* sp. nov.

*Eumyarion beyderensis* differs from *E. lukasi* by its more inflated cusps, thicker crests and by the m1 having an anterior arm of the protoconid. It differs from *E. aegeaniensis* sp. nov. by its more inflated cusps, simpler pattern, absence of anterior and posterior paracone spur, having a short protolophule, by its mesoloph not being connected to the metacone and posterior arm of the protoconid and the mesolophid not being connected in m1.

*Eumyarion beyderensis* differs from *E. bifidus* by mesolophs not connected to the metacone and by having a single protolophule in M2.

### Description

**M1.** The anterocone is large and bicuspid. The labial anteroloph is absent. The lingual anteroloph descends to the protocone. The anterolophule is connected to the protocone. The anterior arm of the protocone ends free in the anterosinus. The posterior paracone spur is present in one specimen and it is connected to the mesoloph. The mesoloph is long and ends free at the labial edge. The ectomesoloph is present in two out of four specimens. The entoloph is longitudinal. While the protolophule is directed posteriorly, the metalophule is directed anteriorly. The posteroloph is long and it is not connected to the metacone. The sinus is wide, directed anteriorly. The molar has three roots.

**M2.** The lingual anteroloph is very weak. The labial anteroloph is strong and ends free. The protolophule is double in one out of eight specimens. The single protolophule is directed anteriorly in one and transverse in four specimens. The protolophule is not visible in the two remaining specimens because of the stage of the wear. The mesoloph is of medium length in four, long and free ending to the labial side in four molars. The posterior paracone spur is present in six, in three of which it is connected to the mesoloph. The ectomesoloph is absent. The metalophule is transverse or slightly directed anteriorly. The posteroloph is separated from the metacone in early stages of wear, it is slightly connected to the metacone in worn specimens. The sinus is directed anteriorly. The roots are not preserved.

**M3.** The labial anteroloph is long and ends free. The lingual anteroloph is absent. The protolophule is double in one specimen, being connected to the anterior part of the protocone and the mesoloph. The single protolophule is transverse and connected to the anterior part of the protocone. The mesoloph is of medium length in two specimens, long and connected to the labial edge in the other three molars. The metalophule is complete. The sinus is open in three out of five specimens. The roots are not preserved.

**m1.** The anteroconid is wide and situated either close to the metaconid or placed medially. The labial anterolophid descends to the protoconid. The lingual anterolophid is short. The anterolophid is absent in five specimens and incomplete in the four others. The weak metalophid is directed anteriorly. The posterior arm of the protoconid and the mesolophid are of medium length and these are not connected to each other. The ectomesolophid is absent in two out of nine specimens. The hypolophid is directed anteriorly. The posterior arm of the hypoconid is long, but it is not connected to the posterolophid in unworn specimens. The sinusid is wide. The molar has two roots.

**m2.** The labial and the lingual anterolophids are well developed. The single metalophid is directed anteriorly and connected to the anterolophid and the lingual anterolophid. The posterior arm of the protoconid and the mesolophid are the same length in one, but the mesolophid is longer in the other specimen. The posterior arm of the protoconid and the mesolophid are not connected. The ectomesolophid is present. The sinusid is wide. The labial mesocingulid is well developed. The posterior arm of the hypoconid ends free. The molar has two roots.

**m3.** The labial and the lingual anterolophids are well developed. The metalophid is single and connects to the lingual anterolophid. The posterior arm of the protoconid is connected to the entoconid. The mesolophid is absent. The ectomesolophid is weak. The labial mesocingulid is well developed. The molar has two roots.

Remarks: The discussions of all *Eumyarion* species are given below.

*Eumyarion aegeaniensis* sp. nov.

Figure 4

**Derivatio nominis.** After the Aegean Sea which is close to the type locality, western Anatolia, Turkey.

**Holotype.** Right M1(PV13593, 1.94 × 1.32), Figure 4B

**Type locality.** Beydere 3 (Manisa/Turkey)

**Age.** Early Miocene, local zone D (MN3)

**Material.** 23 M1 (PV13541, PV13583 – PV13596, PV13650 – PV13657), 17 M2 (PV13547, PV13573, PV13597 – PV13607, PV13658 – PV13661), 13 M3 (PV13608 – PV13616, PV13662 –



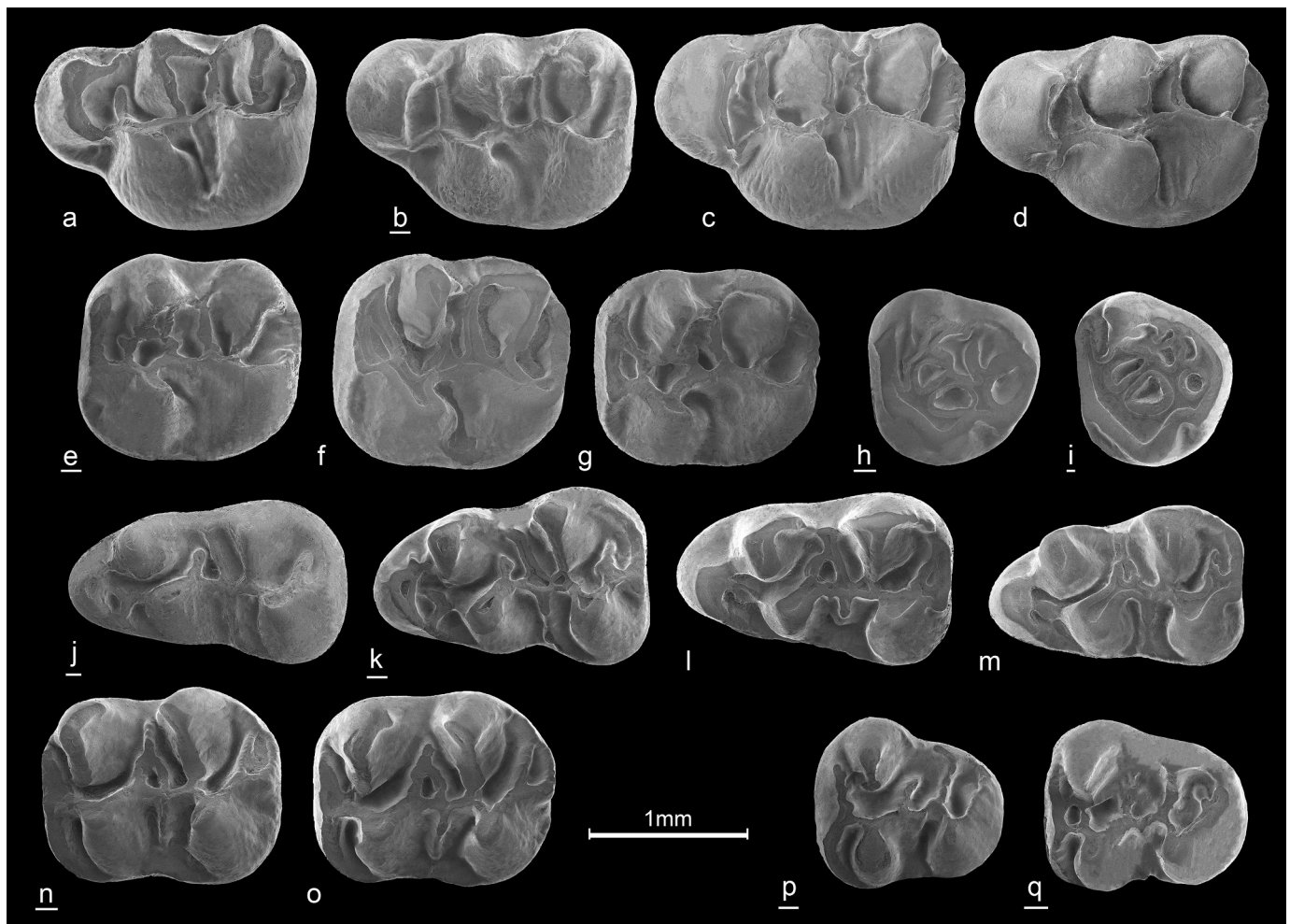


**Figure 4.** *Eumyarion aegeaniensis* sp. nov. (A) M1 sin (PV13588), (B) M1 dex (PV13593), (C) M1 sin (PV13595), (D) M1 sin (PV13656), (E) M2 dex (PV13604), (F) M2 sin (PV13597), (G) M2 sin (PV13607), (H) M3 dex (PV13612), (I) M3 dex (PV13615), (J) m1 dex (PV13626), (K) m1 dex (PV13619), (L) m1 sin (PV13624), (M) m1 sin (PV13667), (N) m2 dex (PV13631), (O) m2 sin (PV13640), (P) m3 dex (PV13644), (Q) m3 dex (PV13647).

PV13665), 14 m1 (PV13532, PV13555, PV13617 – PV13626, PV13666, PV13667) 26 m2 (PV13562 – PV13564, PV13576, PV13579, PV13627 – PV13643, PV13668 – PV13671), 11 m3 (PV13566 – PV13568, PV13580 – PV13582, PV13644 – PV13648)

**Measurements.** Measurements of cheek teeth are given in Table 2.

**Diagnosis.** *Eumyarion* of medium size. M1 and M2 with strong posterior paracone spur that connects to the metacone spur and the mesoloph. M1 with a strong labial anteroloph that connects to the paracone and anterior arm of the protocone. M2 with a high proportion of double protolophules. The m1 and the m2 with

a medium or long mesolophid and a strong ectomesolophid. The m1 and the m2 with a mesolophid that connects to the posterior arm of the protoconid; m1 without metalophulid.

**Differential diagnosis.** *Eumyarion aegeaniensis* sp. nov. differs from *E. microps* De Bruijn and Saraç 1991, *E. intercentralis* De Bruijn and Saraç 1991, *E. orhani* De Bruijn et al. 2006, *E. leemanni* (Hartenberger 1965), *E. gordesensis* Peláez Campomanes et al. 2019, *E. carbonicus* De Bruijn and Saraç 1991 and *E. weinfurteri* (Schaub and Zapfe 1953) by its larger size.

*Eumyarion aegeaniensis* sp. nov. differs from *E. margueritae* De Bruijn et al. 2013, *E. montanus* De Bruijn and Saraç 1991, *E. medius* (Lartet 1851), *E. bifidus* (Fahlbusch 1964) and *E. latior* (Schaub and Zapfe 1953) by its smaller size. It overlaps in size with the smaller specimens of *E. lukasi* Joniak et al. 2017 and the smaller specimens of *Eumyarion beyderensis* sp. nov.

*Eumyarion aegeaniensis* sp. nov. differs from *E. lukasi* by its inflated cusps, by M1 having mesolophs connected to the metacone and posterior paracone spur, and by m1 having a posterior arm of the protoconid connected to the mesolophid. It differs from *E. beyderensis* sp. nov. by slender cusps, by the M1 having mesolophs connected to the metacone and posterior paracone spur, by the absence of the metalophulid in the m1. While the hypocone is higher than the protocone in M1 and M2 in *Eumyarion aegeaniensis*, they are of similar height in *E. beyderensis* sp. nov.

**Table 2.** Measurements of *Eumyarion aegeaniensis* sp. nov.

	Length				N	Width			
	min	mean	max	SD		min	mean	max	SD
M1	1.81	1.94	2.09	0.063	21/22	1.26	1.33	1.47	0.058
M2	1.36	1.43	1.55	0.055	17/17	1.23	1.33	1.44	0.069
M3	1.01	1.08	1.18	0.050	12/12	1.06	1.11	1.18	0.038
m1	1.70	1.79	1.92	0.060	13/13	1.05	1.16	1.24	0.053
m2	1.40	1.52	1.63	0.059	25/23	1.13	1.24	1.34	0.052
m3	1.22	1.29	1.37	0.016	10/10	1.05	1.1	1.14	0.028

### Description

**M1.** The anterocone is slender and slightly bicuspid. The lingual anteroloph is present in two out of 23 specimens only. The anterolophule is connected to the protocone. The posterior spur of the labial anterocone and the anterior arm of the paracone are connected. The anterior arm of the protocone is long and connects to the labial anterocone spur in 21 out of 23 of the M1. The mesoloph is curved posteriorly and connected to the metacone spur. The posterior paracone spur is connected to the metacone spur and the mesoloph. The mesoloph is always connected to the labial edge. The ectomesoloph is present in 16 out of 23 specimens. The protolophule is directed anteriorly. The metalophule is transverse in five, directed anteriorly in 18 specimens. The posteroloph is strong and connects to the metacone. The molar has three roots.

**M2.** The labial anteroloph is strong, while the lingual anteroloph is weak, descending to the base of the protocone. The protolophule is double in all but three molars. There is an extra ridge directed from the protocone to the labial anteroloph in five specimens. The mesoloph is long. The posterior paracone spur is connected to the metacone spur and these two spurs connect to the mesoloph. The ectomesoloph is present in seven out of 17 specimens. The metalophule is directed anteriorly. The posteroloph is connected to the base of the metacone. The sinus is directed anteriorly. The molar has three roots.

**M3.** While the lingual anteroloph is very weak in eight molars and absent in five, the labial anteroloph is always well developed. The protolophule is always double. The anterior protolophule is directed transversely in five specimens and directed anteriorly in the other eight. The posterior paracone spur is weak. The mesoloph is always connected to the labial ridge. The neontoloph is present. A shallow sinus is present. The molar has three roots.

**m1.** The labial anterolophid is well developed and descends to the protoconid. The lingual anterolophid is present in five molars and absent in nine. The anterolophid is connected to the protoconid in all specimens with the exception of one, in which it is incomplete. The labial spur of the anterolophid is present in seven out of 13 specimens. The metaconid and the anteroconid

connection is complete. The metalophule is absent. The mesolophid is always connected to the lingual ridge. The posterior arm of the protoconid is variable. It is shorter than the mesolophid and ends free in five specimens, it is connected to the metaconid in two and connected to the mesolophid in the other seven molars. The ectomesolophid is always present. The very short hypolophid is directed anteriorly. The posterior arm of the hypoconid is always present and it is connected to the posterolophid in seven out of 13 specimens. The labial mesocingulid is present in all specimens but one. The molar has two roots.

**m2.** The labial and the lingual anterolophids are well developed. The metalophid and the hypolophid are directed anteriorly. The posterior arm of the protoconid and the mesolophid are connected in the middle and continue to the lingual edge as a single lophid in 18 of the 23 molars. The posterior arm of the protoconid and the mesolophid are not connected in five specimens and the mesolophid is absent in three molars. The ectomesolophid is present in all but one molar. The posterior arm of the hypoconid is always connected to the posterolophid. The sinusid is wide and the labial mesocingulid is present. The molar has two roots.

**m3.** The labial anterolophid is well developed, while the lingual anterolophid is short. The metalophid has become integrated with the lingual anterolophid. The posterior arm of the protoconid is connected to the lingual ridge. The mesolophid is absent. The ectomesolophid is present in all specimens. The molar has two roots.

Remarks: The discussions of all *Eumyarion* species are given below.

*Eumyarion* sp.

### Figure 5

**Material and measurement.** 4 M1 (PV13523,  $1.83 \times 1.31$ ; PV13524,  $1.84 \times 1.40$ ; PV13570,  $1.80 \times 1.37$ ; PV13572,  $1.78 \times 1.32$ ), 1 M2 (PV13527,  $1.40 \times 1.31$ ) 2 M3 (PV13528,  $1.05 \times 1.04$ ; PV13529,  $1.00 \times 1.05$ ), 3 m1 (PV13530,  $1.74 \times 1.07$ ; PV13531,  $1.60 \times 0.96$ ; PV13571, - x -), 1 m2 (PV13533,  $1.34 \times 1.04$ ), 2 m3 (PV13535,  $1.15 \times 1.08$ ; PV13536,  $1.17 \times 1.00$ )

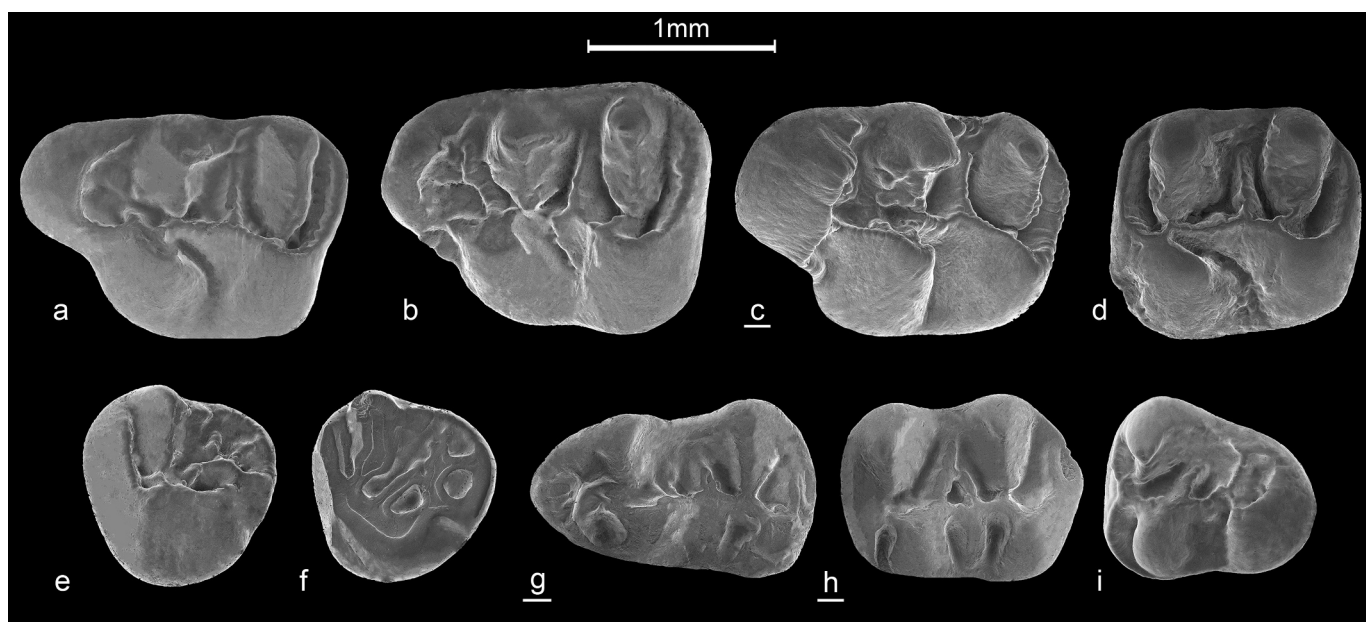


**Figure 5.** *Eumyarion* sp. (A) M1 sin (PV13523), (B) M1 sin (PV13570), (C) M1 dex (PV13524), (D) M2 sin (PV13527), (E) M3 sin (PV13529), (F) M3 sin (PV13528), (G) m1 dex (PV13530), (H) m2 dex (PV13533), (I) m3 sin (PV13536).

### Description

**M1.** The anterocone is rounded anteriorly in two specimens and angled in the other. The anterior valley displays a number of characteristic, irregular thin ridges, which originate from the anterocone, the protocone and the paracone. The lingual anteroloph descends to the base of the protocone in two molars and it is absent in the other two M1. The labial anteroloph is present in three specimens, but absent in one. The anterolophule is connected to the protocone. The very short protolophule is directed posteriorly. The posterior paracone spur is present in two out of four specimens. The mesoloph is long. The metalophule is curved anteriorly. The ridges are slender. The sinus is directed anteriorly. The roots are not preserved.

**M2.** The lingual anteroloph is weak. The labial anteroloph is strong and connected to the paracone. The single protolophule is directed posteriorly. The mesoloph is of medium length. The posterior paracone spur is present and it is not connected to the mesoloph. The ectomesoloph is absent. The metalophule is directed anteriorly. The posteroloph is connected to the metacone. The sinus is directed anteriorly. The roots are not preserved.

**M3.** The lingual anteroloph is present in one and absent in the other specimen. The protolophule is single. It is directed anteriorly in one and transverse in the other specimen. The posterior paracone spur is absent. The mesoloph is of medium length in one and connected to the labial border in the other molar. The neoentoloph is present. The metalophule is short. A very shallow sinus is present. The roots are not preserved.

**m1.** The cusps and ridges are slender. The anteroconid is rounded and significantly smaller than the other conids. The labial anterolophid is comma-shaped and descends to the protoconid. The lingual anterolophid is very short and connects to the metaconid. The anterolophulid is incomplete in one specimen and absent in two. The metalophulid is absent in one specimen and connected to the protoconid in the other two specimens. The mesoloph is of medium length. The posterior arm of the protoconid is absent or very weak. The ectomesolophid is present in all specimens. The labial cingulum is well developed. The hypolophulid is directed anteriorly. The posterior arm of the hypolophulid is weak. The sinusid is wide. The roots are not preserved.

**m2.** The cusps and ridges are slender. The labial anterolophid descends to the protoconid. The lingual anterolophid is connected to the metaconid. The metalophulid and the anterior arm of the protoconid are connected to the lingual anterolophid. The posterior arm of the protoconid reaches to the lingual ridge. The mesolophid is of medium length and connects to the posterior arm of the protoconid. The ectomesolophid is present. The posterior arm of the hypoconid is connected to the posterolophid. The roots are not preserved.

**m3.** The labial and lingual anterolophids are well developed. The metalophulid is directed anteriorly and connected to the lingual anterolophid. The posterior arm of the protoconid is of medium length. The mesolophid is absent. The ectomesolophid is very weak. The roots are not preserved.

### Discussion

The evolutionary history of *Eumyarion* is complex and largely still unresolved. Especially *Eumyarion* of medium size from the early Miocene of Anatolia show a mosaic of what are considered to be derived dental characteristics (De Bruijn and Saraç 1991) and a high degree of endemism (e.g., De Bruijn et al. 2006; Joniak et al. 2019; Pelaez-Campomanes et al. 2019). This makes it very complicated to reconstruct evolutionary lineages.

We found three species of *Eumyarion* from Beydere 3, which is usual in the early Miocene of Anatolia, as the same number is recognised from Sabuncubeli and Harami 4 as well (De Bruijn et al. 2006; Joniak et al. 2019). However, in contrast to the latter two assemblages, Beydere 3 has two *Eumyarion* species with a similar lower dentition and similar size. This situation is also known from the locality Schönweg-‘Brüchl’ in Austria and Sandelzhöhen in Germany, where *Eumyarion bifidus* and *E. weinfurteri* co-occur (De Bruijn 2009; Prieto et al. 2016). De Bruijn (2009) suggested that species with similar size and morphology could occur together if they are adapted to a specific food source occurring in the same biotope. Alternatively, the species could prefer a somewhat different biotope in the same region, avoiding competition in that way. On the other hand, the *Eumyarion* assemblage from Oberdorf largely has characteristics of *E. weinfurteri* but already shows some *E. bifidus* characters in a small part of the assemblage. Therefore, *Eumyarion* from Oberdorf has been assigned to *E. aff. weinfurteri* (Daxner-Höck 1998).

Among the three *Eumyarion* species from Beydere 3, *Eumyarion* sp. is the rarest. It is very characteristic with a crenulated anterosinus in M1, less developed or absent anterior arm of the protocone, medium length of the mesoloph that is not connected to either posterior arm of the paracone nor the metacone, incomplete or absent anterolophulid as well as a short mesolophid and posterior arm of the protoconid. This is similar to the morphological pattern observed in *Eumyarion gordesensis*. However, *E. gordesensis* from Gördes has a small number of elements that show a lot of variation. Also, *E. gordesensis* and *Eumyarion* sp. do not intersect biostratigraphically and *Eumyarion* sp. is larger than *E. gordesensis*. Since the material is very limited and there are no direct equivalents, we prefer to keep the Beydere species in open nomenclature, for now.

*Eumyarion beyderensis* is the second dominant *Eumyarion* in the assemblage. The dental morphology of the species is characterised by inflated cusps and thick crests. Although *Eumyarion beyderensis* overlaps metrically with *Eumyarion aegeaniensis*, the average size is larger. *Eumyarion beyderensis* shows a simpler morphology by having incomplete or absent anterior paracone and posterior metacone spur, a single protolophule, incomplete or absent anterolophulid, short mesolophid and short posterior arm of the protoconid. Although Anatolian early Miocene localities are very diverse with the species of *Eumyarion*, only *E. montanus* has a similar morphology to *E. beyderensis*. However, *E. beyderensis* is smaller than *E. montanus*. It has more inflated cusps and thicker crests.

*Eumyarion aegeaniensis* is the dominant species in the fauna. It is very characteristic with a complex crest pattern. Morphologically, it displays such a long anterior arm of the protocone that it is connected with the anterior paracone spur, while the long mesoloph is connected with the posterior paracone spur and the metacone in M1 and M2. This basal morphology is also observed in *Eumyarion orhani* and *E. bifidus*. According to De Bruijn et al. (2006), *E. orhani* from Sabuncubeli could be ancestral to *E. bifidus*, assuming an increase in size, while preserving the main characters of the morphology. *Eumyarion aegeaniensis* from Beydere 3 is larger than *E. orhani* and smaller than *E. bifidus* (Figure 6). It has more developed crests and larger cusps than *E. orhani*. The stratigraphic order of these three species supports the intermediate morphology of *Eumyarion aegeaniensis* in the overall trend as well. Nevertheless, in spite of the shared morphology between these *Eumyarion* species, it is still difficult to firmly establish their phylogenetic relationships. A comprehensive study,



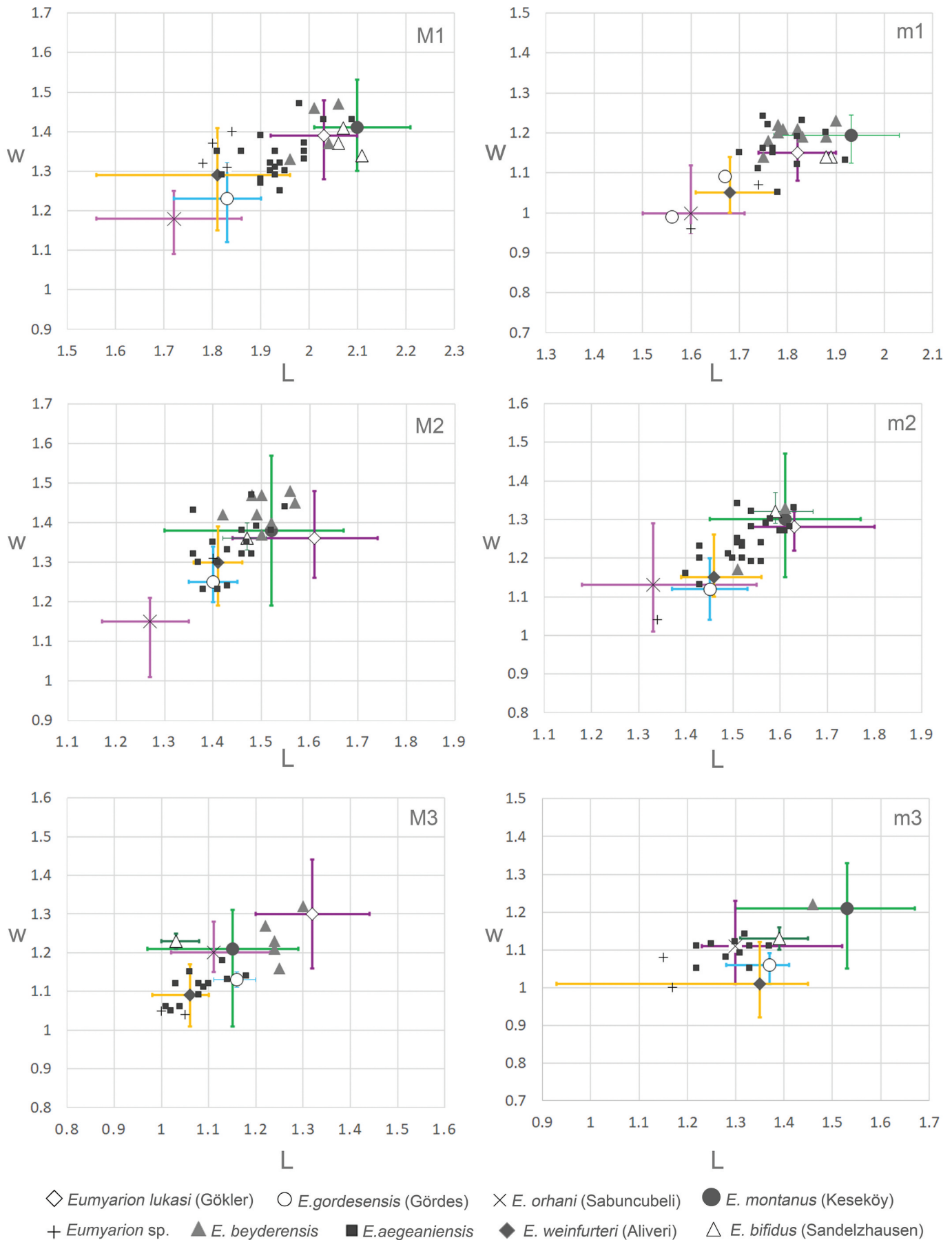


**Figure 6.** Scatter diagram of length (L) and width (W) of the upper and lower molars of *Eumyarion* species from Anatolia and Europe. The data after Klein Hofmeijer and de Bruijn 1988; De Bruijn and Saraç 1991; De Bruijn et al. 2006; De Bruijn 2009; Joniak et al. 2017; Pelaez-Campomanes et al. 2019

including cladistic and geometric morphometric analysis would be needed to reconstruct the detailed evolutionary story of *Eumyarion*.

Genus *Megacricetodon* Fahlbusch 1964

*Megacricetodon hellenicus* Oliver and Pelaez-Campomanes 2014

Figure 7 A–M

**Material.** 7 M1 (PV13410 – PV13415, PV13450), 5 M2 (PV13416 – PV13419, PV13451), 10 M3 (PV13420 – PV13427, PV13452, PV13453), 11 m1 (PV13428 – PV13435, PV13454 – PV13456), 4 m2 (PV13436 – PV13439), 8 m3 (PV13440 – PV13446, PV13457).

**Measurements.** Measurements of cheek teeth are given in Table 3.

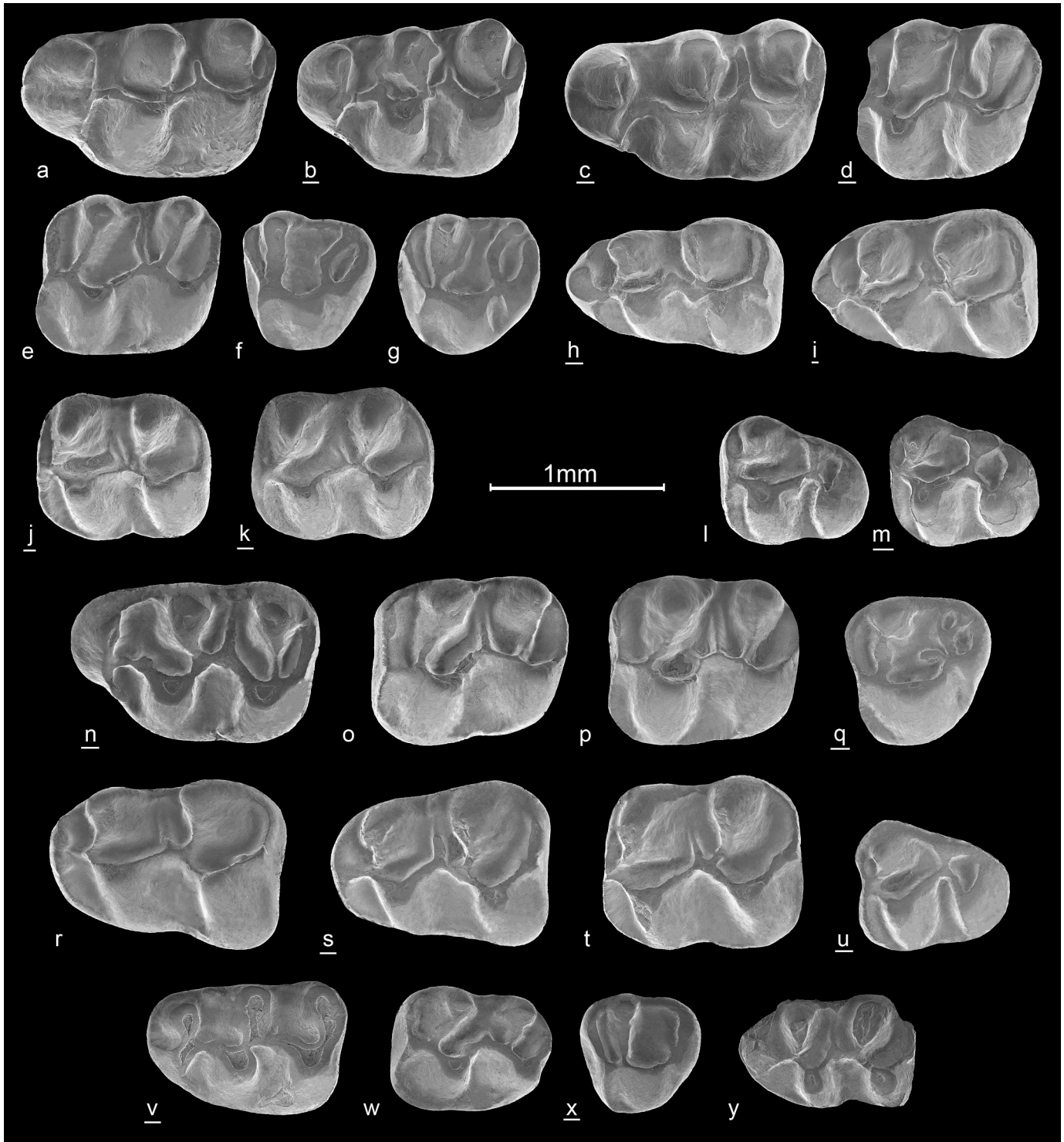


**Figure 7.** *Megacricetodon hellenicus* (A) M1 sin (PV13414), (B) M1 dex (PV13412), (C) M1 dex (PV13450), (D) M2 dex (PV13417), (E) M2 sin (PV13451), (F) M3 sin (PV13421), (G) M3 sin (PV13424), (H) m1 dex (PV13433), (I) m1 dex (PV13431), (J) m2 dex (PV13436), (K) m2 dex (PV13437), (L) m3 sin (PV13445), (M) m3 dex (PV13442); *Democricetodon doukasi* (N) M1 dex (PV13460), (O) M2 sin (PV13506), (P) M2 sin (PV13504), (Q) M3 dex (PV13473), (R) m1 sin (PV13475), (S) m1 dex (PV13480), (T) m2 sin (PV13485), (U) m3 dex (PV13491); *Vallaris zappai* (V) M1 dex (PV13400), (W) M2 sin (PV13402), (X) M3 dex (PV13406), (Y) m1 sin (PV13407).

**Table 3.** Measurements of *Megacricetodon hellenicus*.

	Length					Width			
	min	mean	max	SD	N	min	mean	max	SD
M1	1.41	1.46	1.53	0.051	4/5	0.94	0.98	1.02	0.025
M2	1.02	1.05	1.08	0.024	5/5	0.93	0.97	1.03	0.044
M3	0.73	0.78	0.84	0.035	9/9	0.75	0.81	0.86	0.035
m1	1.20	1.28	1.35	0.054	9/9	0.80	0.87	0.91	0.029
m2	1.02	1.09	1.12	0.040	4/4	0.75	0.88	0.94	0.077
m3	1.04	0.94	0.87	0.048	8/8	0.72	0.77	0.86	0.049

### Description

**M1.** The anterocone is slightly divided. A small platform is present in front of the furrow in four out of seven specimens. The labial anterocone is larger than the lingual anterocone. The labial anterostyl is present. The anterolophule is connected to the lingual anteroloph. The labial spur of the anterolophule is absent. The protolophule is double in two specimens and single in the other five. The single protolophule is directed posteriorly. A very weak posterior paracone spur is present in two specimens. The lingual mesocingulum is present in all specimens. The mesoloph is long and reaches the labial border in three specimens and is of medium length in four. The metalophule is directed posteriorly and connected to the posteroloph. The posteroloph is short. The sinus is transverse. The molar has three roots.

**M2.** The lingual anteroloph descends to the base of the protocone. The labial anteroloph is connected to the paracone. The protolophule is double in two specimens and single in the other three. The single protolophule is directed anteriorly and connected to the anterior arm of the protocone. The posterior arm of the protocone is longer than the anterior arm of the hypocone. The mesoloph is long and connected to the labial border in all specimens. The posterior paracone spur is weak; it is connected with the mesoloph in two specimens. The metalophule is directed anteriorly in all specimens. The sinus is transverse. The roots are not preserved.

**M3.** The lingual anteroloph is weak and developed as a small ledge at the anterolingual base of the protocone. The labial anteroloph is well developed and connected to the paracone. The protolophule is well developed. It is connected to the anterolophule. The metalophule and the anterior arm of the hypolophule connect in the centre of the posterosinus. The metacone is distinguishable in three and it is fused with the posteroloph in seven specimens. The sinus is weak or absent. The molar has three roots.

**m1.** The anteroconid is simple, rounded. The labial and the lingual anterolophids descend to the protoconid and the metaconid, respectively. The metalophulid is directed anteriorly and connected to the anterolophulid. The anterolophulid is placed in the middle and connected to the protoconid. The mesolophid is absent in three and of medium length in eight molars. The very short hypolophulid is always directed anteriorly. The labial mesocingulid is present in all specimens. The posterior sulcus is present in three specimens. The sinusid is wide. The molar has two roots.

**m2.** The labial anterolophid is long and descends to the base of the protoconid. The lingual anterolophid is very weak. The metalophulid is directed anteriorly. The labial mesocingulid is present. The mesolophid is of medium length. The hypolophulid is always directed anteriorly. The posterolophid is strong and connects to the entoconid. The posterior sulcus is present in one specimen. The sinusid is directed anteriorly. The roots are not preserved.

**m3.** The labial anterolophid is long and descends to the base of the protoconid. The lingual anterolophid is shorter and connected to the metaconid. The metalophulid is directed anteriorly. It is merged with anterolophulid in two specimens as a result of the stage of the wear. The mesolophid is absent. The sinusid is transverse. The molar has two roots.

**Remarks.** Species of *Megacricetodon* are not well known during the early Miocene of Anatolia. The oldest occurrence is *Megacricetodon* sp. from Keseköy (Zone D/MN3) (Wessels et al. 2001) and otherwise it is known by *M. primitivus* from Çapak (Zone E/MN4) (Bilgin et al. 2021). The Beydere 3 specimens overlap metrically with the smaller specimens of *Megacricetodon* sp. from Keseköy. *Megacricetodon* sp. also differs in having inflated cusps, a deeply split anterocone and having a posterior paracone spur on the M1 and M2. *Megacricetodon primitivus* from Çapak is much smaller than the Beydere 3 specimens.

*Megacricetodon hellenicus* is only known from the Greek locality of Aliveri (MN4). Besides having a similar morphology, our specimens metrically overlap with *M. hellenicus* from the Greek locality or are slightly larger (Figure 8). However, this may be explained by the small sample size of Aliveri. Since the dental pattern fits well, we assign our specimens to *Megacricetodon hellenicus*. Therefore, the

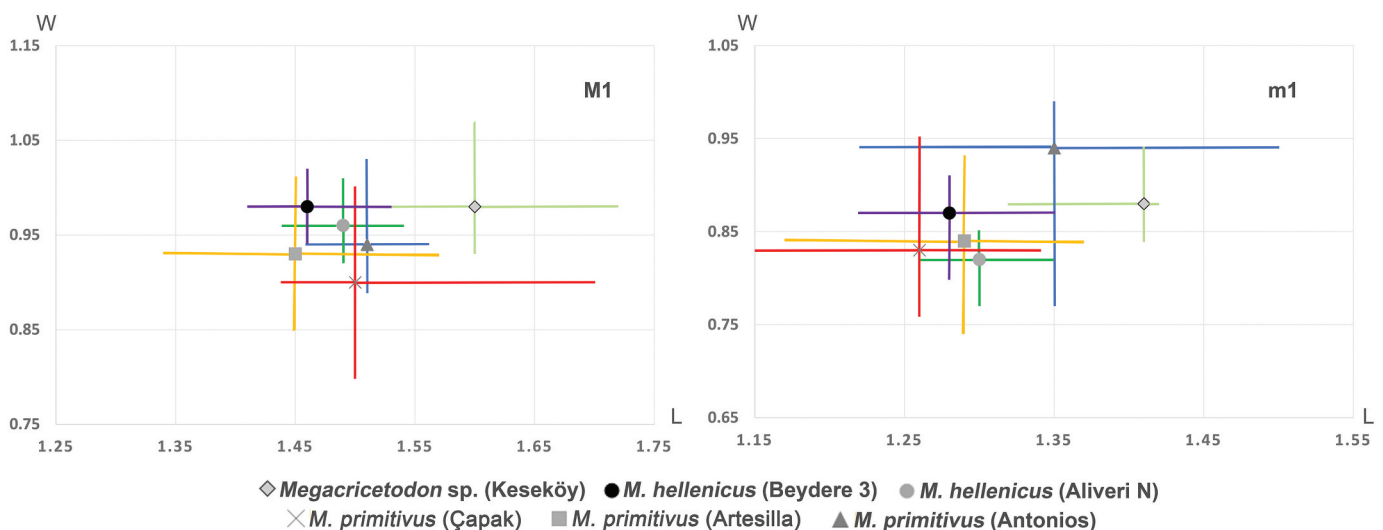


**Figure 8.** Scatter diagram of length (L) and width (W) of the upper and lower molars of *Megacricetodon* species from Anatolia and Europe. The data after Wessels et al. 2001; Oliver and Pelaez-Campomanes 2014; Bilgin et al. 2021; Vasileiadou and Koufos 2005



presence of *M. hellenicus* in Beydere 3 assemblage expands the range geographically to Anatolia and stratigraphically to the local zone D (MN3).

Genus *Democricetodon* Fahlbusch 1964

*Democricetodon doukasi*; Theocharopoulos 2000

Figure 7 N–U

**Material.** 8 M1 (PV13460 – PV13463, PV13495 – PV13498), 16 M2 (PV13464 – PV13470, PV13499 – PV13507), 4 M3 (PV13471 – PV13474), 10 m1 (PV13475 – PV13480, PV13509 – PV13512), 12 m2 (PV13481 – PV13487, PV13513 – PV13517), 8 m3 (PV13488 – PV13494, PV13518)

**Measurements.** Measurements of cheek teeth are given in Table 4.

**Table 4.** Measurements of *Democricetodon doukasi*.

	Length				N	Width			
	min	mean	max	SD		min	mean	Max	SD
M1	1.48	1.55	1.61	0.043	7/8	0.98	1.04	1.13	0.048
M2	1.06	1.13	1.19	0.045	16/15	1.00	1.03	1.09	0.034
M3	0.79	0.84	0.90	0.042	4/4	0.77	0.83	0.88	0.042
m1	1.28	1.33	1.40	0.034	10/10	0.88	0.96	0.99	0.030
m2	1.12	1.17	1.24	0.030	11/11	0.94	0.98	1.05	0.032
m3	0.93	1.00	1.08	0.057	5/5	0.75	0.80	0.85	0.036

### Description

**M1.** The labial side of the anterocone is higher than the lingual side. The labial anteroloph is connected to the paracone. The lingual anteroloph is connected to the base of the protocone. The anterolophule is connected to the anterocone lingually. The lingual spur of the anterolophule is present in one specimen. The protolophule is single and directed posteriorly in six and double in two specimens. The mesoloph is of medium length in four; it is long and connected to the labial margin in the other four specimens. A weak posterior paracone spur is present in one specimen. The labial mesocingulum is present in all specimens. The metalophule is directed posteriorly in four and transversely in the other four specimens. The sinus is transverse. The molar has three roots.

**M2.** The labial and lingual anterolophs are well developed in all but one specimen, in which the labial anteroloph is very low and weak. The lingual anteroloph descends to the base of the protocone. The labial anteroloph is connected to the paracone. The protolophule is double in seven specimens and single and directed anteriorly in nine specimens. The mesoloph is of medium length in five molars; it is long and connected to the labial margin in eleven specimens. The posterior paracone spur is present in all but three molars. It is connected to the mesoloph in ten specimens. The labial and the lingual mesocingulum is present. The metalophule is directed anteriorly in eleven, directed posteriorly in one and transverse in four specimens. The posteroloph is well developed. The molar has three roots.

**M3.** The lingual anteroloph is weak and forms a small ledge at the anterolingual base of the protocone. The labial anteroloph is well developed and connects to the paracone. The metacone is weak. The mesoloph is absent in one molar. The metacone and the hypocone are connected by the anterior arm of the hypocone, the metalophule and the posteroloph. The sinus is shallow. The molar has three roots.

**m1.** The anteroconid is simple. The labial anterolophid is longer than the lingual anterolophid. The labial and lingual anterolophid descend to the base of the protoconid and to the metaconid, respectively. The metalophulid and the anterior arm of the protoconid are connected with the anterolophulid. The metalophulid is always single and directed anteriorly. The mesolophid is connected to the lingual margin in four and of medium length in five specimens. The ectomesolophid is present in two specimens. The hypolophulid is double in one, single and directed anteriorly in eight molars. The posterolophid is well developed. The posterior sulcus is absent in three specimens. The mesostylid is present in one molar. The molar has two roots.

**m2.** The labial anterolophid descends to the base of the protoconid. The lingual anterolophid is very weak. It connects to the metaconid in seven and is absent in five molars. The metalophulid is single and directed anteriorly in eleven specimens and double in one. The mesolophid is connected to the lingual border in four and of medium length in eight molars. The hypolophulid is directed anteriorly. The posterolophid is well developed and the posterosinusid is closed. The sinusid is wide and directed anteriorly. The molar has two roots.

**m3.** The lingual anterolophid is shorter than the labial anterolophid in most of the specimens. The labial anteroloph is well developed and descends to the base of the protoconid. The mesosinusid is well developed. The metalophulid is directed anteriorly in five specimens and transversely in one. The mesolophid is absent in all but one specimen. The sinusid is transverse. The molar has two roots.

### Remarks

*Democricetodon doukasi* is known from its type locality Keseköy described by Theocharopoulos (2000) and from Sabuncubeli described by De Bruijn et al. (2006). The finds from Gördes and Harami 5 were described as *Democricetodon* cf. *doukasi* (Joniak et al. 2019; Peláez-Campomanes et al. 2019). *Democricetodon* specimens from Beydere 3 are metrically within the variation of *D. doukasi* from Keseköy and Sabuncubeli. The assemblage from Keseköy is characterised by a well-developed posterior paracone spur in the M1 and M2. The posterior paracone spur is present in M2, but it is weak or absent in M1 for *Democricetodon* from Beydere 3, as it also is in the assemblage from Sabuncubeli. The reason for this similarity may lie in the geographical proximity of Sabuncubeli and Beydere 3, in which case it would represent regional variation. Apart from the development of the posterior paracone spur, *Democricetodon* from Beydere 3 shows the same characters as *D. doukasi* from Keseköy.

Genus *Vallaris* Wessels, Theocharopoulos, De Bruijn and Ünay 2001

*Vallaris zappai* Wessels, Theocharopoulos, De Bruijn and Ünay 2001

Figure 7 V–Y

**Material and measurement.** 1 M1 (PV13400, 1.18 × 0.81), 5 M2 (PV13401, 0.92 × 0.74; PV13402, 0.91 × 0.76; PV13403, 0.93 × 0.75; PV13404, 0.93 × 0.78; PV13405, 0.85 × 0.71), 1 M3 (PV13406, 0.73 × 0.76), 1 m1 (PV13407, 0.96 × 0.65)

### Description

**M1.** The labial cusp of the anterocone is slightly larger than the lingual cusp. There is a small platform in front of the anterocone. The labial anterostyl is present. The anterolophule is connected to the lingual anterocone. The protolophule is single and directed posteriorly. The posterior paracone spur is absent. The mesoloph is short. The posteroloph is fused with the metalophule. The entostyl is present close to the base of the hypocone. The sinus is directed anteriorly. The roots are not preserved.

**M2.** The anteroloph is equally developed. The lingual anteroloph descends to the base of the protocone and the labial one is connected to the paracone. The protolophule and the metalophule are single and directed anteriorly. The mesoloph is short in two and long in three specimens. The ectomesoloph is absent. The posteroloph is strong and connected to the base of the metacone. A weak entostyl is present in one specimen. The sinus is wide and directed anteriorly. The molar has three roots.

**M3.** The lingual anteroloph is weak and forms a small ledge at the anterolingual base of the protocone. The labial anteroloph is well developed. The protolophule is transverse and connected to the anterior arm of the protocone. The metalophule and the metacone are absent. A strong posteroloph descends along the entire posterolingual margin to the base of the paracone. The anterior arm of the hypocone ends free in the posterosinus. The mesoloph is absent. The roots are not preserved.

**m1.** The anteroconid is small and conical. The part of the lingual anterolophid is broken. The position of anterolophulid is closer to the metaconid. The metalophulid is very short, directed anteriorly and connected to the anterolophulid. The mesolophid is of medium length. The mesostylid is present. A very short hypolophulid is directed anteriorly. The posterolophid is well developed. The sinus is wide. The roots are not preserved.

#### Remarks

The genus *Vallaris* is only known from the species *Vallaris zappai*. The species is endemic to Anatolia and known from a very specific time range (local zone D), so far. The species is described from the type locality of Keseköy and Sabuncubeli (Wessels et al. 2001; De

Brujin et al. 2006). The size and morphology of the specimens from Beydere 3 are within the variation of *Vallaris zappai* from its type locality.

Family Gliridae Muirhead 1819

Genus *Glirulus* Thomas 1906

*Glirulus ekremi* Ünay 1994

Figure 9 A–L

**Material.** 6 M1/2 (PV13370 – PV13373, PV13389, PV13390), 1 M3 (PV13375), 3 p4 (PV13376, PV13391, PV13392), 6 m1 (PV13377 – PV13381, PV13394), 6 m2 (PV13382 – PV13384, PV13393, PV13395, PV13396), 7 m3 (PV13385 – PV13388, PV13396, PV13397)

**Measurements.** Measurements of cheek teeth are given in Table 5.

**Table 5.** Measurements of *Glirulus ekremi*.

	Length					Width			
	min	mean	max	SD	N	min	mean	max	SD
M1-2	0.88	0.93	0.98	0.033	6/6	1.02	1.05	1.08	0.024
M3	-	0.89	-	-	1/1	-	0.79	-	-
p4	0.77	0.78	0.79	-	3/3	0.69	0.70	0.71	-
m1	0.86	0.93	1.01	0.051	5/5	0.74	0.89	1.00	0.074
m2	0.99	1.03	1.10	0.040	5/4	1.01	1.06	1.10	0.033
m3	0.86	0.91	0.97	0.036	7/7	0.82	0.87	0.95	0.036

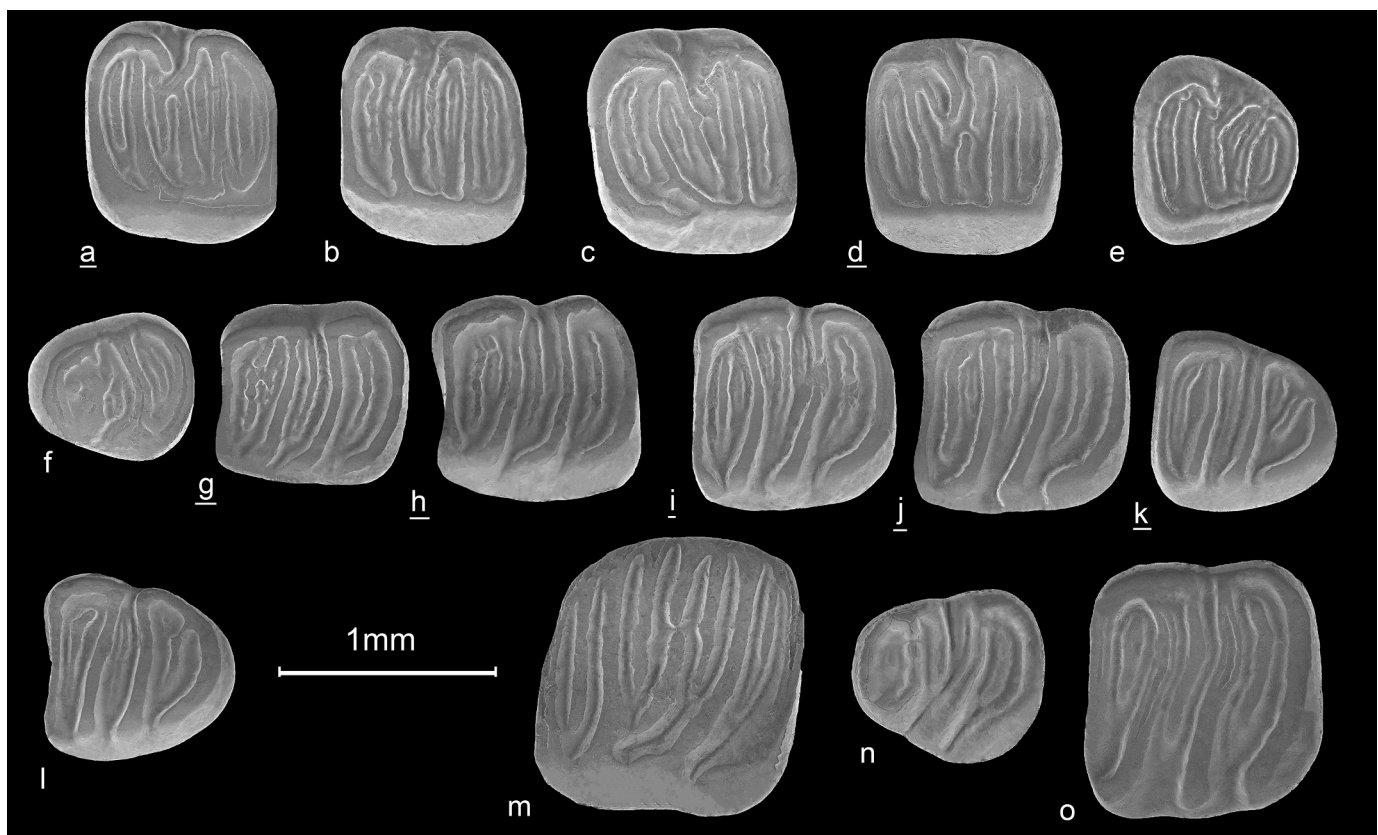


**Figure 9.** *Glirulus ekremi* (A) M1/2 dex (PV13371), (B) M1/2 sin (PV13373), (C) M1/2 sin (PV13390), (D) M1/2 dex (PV13372), (E) M3 sin (PV13375), (F) p4 sin (PV13376), (G) m1 dex (PV13377), (H) m1 dex (PV13394), (I) m2 dex (PV13393), (J) m2 dex (PV13382), (K) m3 dex (PV13386), (L) m3 sin (PV13397); *Glis* sp. (M) M1/2 sin (PV13520), (N) sin (PV13521), (O) m1 sin (PV13522).

### Description

**M1/2.** The occlusal surface of the molar is concave. The number of ridges is nine in all specimens. The four main ridges are connected by the endoloph. The anteroloph, the protoloph and the anterior centroloph are connected in the paracone area, while the posterior centroloph, the metaloph and the posteroloph are connected in the metacone area. The posterior centroloph is longer than anterior centroloph. The extra ridges are long and occupy almost the entire length of valleys. The roots are not preserved.

**M3.** The occlusal surface of the molar is concave. The molar has nine ridges. The four main ridges are connected by an endoloph. The anterior centroloph and the posterior centroloph merge in the centre and end free as one loph. While the labial connection is present in the metaloph, it is absent in the anterior extra ridge and the protoloph. The roots are not preserved.

**p4.** The outline of the molar is sub-triangular and the occlusal surface is flat. The premolars have seven ridges in two and eight ridges in one specimen. The anterior extra ridge is very small and weak. The centrolophid is of medium length and ends free. There is an extra ridge in the central valley in one out of three specimens. The posterior extra ridge is present in all specimens. The roots are not preserved.

**m1 and m2.** The occlusal surface of the molar is concave. The number of ridges is eight in two molars and nine in the rest of the specimens. The metalophid and the anterolophid are connected on the labial side in three specimens. The anterior and the posterior extra ridges have no connection to the labial or lingual ridge, except for in one specimen. Ten out of 12 specimens have a double anterior extra ridge and it is not visible in two specimens because of the stage of wear. The posterior extra ridge is always single. A very weak central extra ridge is present in four specimens. The centrolophid is long and ends free. The endolophid is present in one m1. The metalophid, the mesolophid and the posterolophid are directed anteriorly along the labial side. The labial end of these ridges is always free. The roots are not preserved.

**m3.** The occlusal surface is slightly concave. The number of ridges is seven in four molars and eight in three. The anterior extra ridge is always single, while the posterior extra ridge is double in four and single in three specimens. The centrolophid is long and always ends free. It is connected to the lingual ridge in five out of seven specimens. The endolophid is present in one out of seven specimens. The roots are not preserved.

### Remarks

The small sized glirid from Beydere 3 shows the characteristic features of the genus *Glirulus* with its concave occlusal surface and semi-complex ridge pattern. De Bruijn (1998) suggested dividing the species of *Glirulus* into the two groups based on anterior extra ridge in m1 and m2. Group A has two extra ridges between the anterolophid and the metalophid and consist of five species *Glirulus japonicus* (Schinz 1845), *G. conjunctus* (Mayr 1979), *G. ekremi* Ünay 1994, *G. lissiensis* (Hugueney and Mein 1965) and *G. pusillus* (Heller 1936). Group B is characterised by having one extra ridges between the anterolophid and metalophid and comprises three species, *G. diremptus* (Mayr 1979), *G. minor* Wu 1993 and *G. daamsi* De Bruijn et al. 2003. *Glirulus* from Beydere 3 fits in group A with two extra ridges between the anterolophid and metalophid.

The species of *Glirulus* are known in Anatolia from the most primitive: *G. aff. ekremi* from Harami 1, *G. ekremi* from Sabuncubeli and Keseköy, *Glirulus* indet. from Söke, *G. daamsi* from Çandır and *G. lissiensis* from Düzyayla (Ünay 1994; Ünay and Göktaş 1999; De Bruijn et al. 2003; Dinçarslan and Suata-Alpaslan 2016). *Glirulus* from Beydere 3 is metrically and morphologically only compatible with *G. ekremi* from Keseköy. However, while the upper molars and m3 have the same morphology as *G. ekremi* from

Keseköy, there are differences on m1 and m2. The differences are mainly the development of the extra ridges. *Glirulus ekremi* from Keseköy has a double anterior extra ridge in m1 and m2 as has *Glirulus* from Beydere 3. However, the second extra ridge is very weak in Beydere 3 specimens. In addition, while the Keseköy specimens have a centrolophid extra ridge in m1 and m2, this crest is only present in one out of eight specimens from Beydere 3.

The differences between the assemblages are not enough to separate Beydere 3 specimens from those of Keseköy and the differences in the morphology of m1 and m2 may be due to ecophenotypic variation. The geographical distance and different depositional environment could account for these possible intraspecific variations.

Genus *Glis* Brisson 1762

*Glis* sp.

Figure 9 M–O

**Material and measurement.** 1 M1/2 (PV13520, 1.24 x ~ 1.26), 1 p4 (PV13521, 0.90 × 0.82) 1 m2 (PV13522, 1.17 × 1.22)

### Description

**M1/2.** The occlusal surface of the molar is slightly concave with nine ridges. The lingual end of the anteroloph is curved posteriorly and ends free. The posterior centroloph is longer than the anterior centroloph. The protoloph, the metaloph and the posteroloph are connected by the endoloph. The three extra ridges (anterior valley extra ridge, trigon anterior extra ridge and posterior valley extra ridge) are long and occupy almost the entire length of valleys. The roots are not preserved.

**p4.** The occlusal surface is flat. Four extra ridges are present. The anterolophid, the metalophid and the centrolophid are connected lingually as are the central valley extra ridge, the mesolophid and the posterolophid. The anterior extra ridge and the posterior extra ridge are both present, the latter one is better developed. The central valley extra ridge is very weak. The roots are not preserved.

**m2.** The occlusal surface is slightly concave. Two extra ridges are present. The anterolophid, the metalophid and the centrolophid are connected lingually as are the mesolophid and the posterolophid. The anterolophid and the metalophid are connected labially as well. The posterior extra ridge is stronger than the anterior extra ridge. The labial ends of anterolophid and mesolophid are transverse, while the metalophid and posterolophid are directed anteriorly.

### Remarks

*Glis* is represented by two different species in Anatolia during the early Miocene. It is known from the most primitive *Glis transversus* Ünay 1994 from Harami 1 and *Glis galitopouli* Van der Meulen and De Bruijn 1982 from Sabuncubeli and Keseköy (1994; De Bruijn et al. 2006). In addition, ?*Glis* indet. Was reported from Kınık 2 (Ünay and Göktaş 2000).

The *Glis* specimens from Beydere 3 are metrically in the range of *G. galitopouli* from its type locality of Aliveri. They both share the same features; such as the anterior and posterior valley extra ridges, having eight lophs in p4, lingually connected protoloph, metaloph and posteroloph for M1/2, as well. However, the m2 from Beydere 3 is different from any *Glis* species by having seven ridges. Because of these inconsistencies and the scarce material, Beydere 3 assemblage is classified as *Glis* sp.

Family Sciuridae Fischer 1817

Genus *Palaeosciurus* Pomel 1853

*Palaeosciurus fissurae* Dehm 1950

Figure 10 A–D



**Material and measurement.** 1 P4 (PV13367,  $1.55 \times 1.89$ ), 1 M1/2 (PV13366,  $1.80 \times 2.10$ ), 1 d4 (PV13368,  $1.51 \times 1.40$ ), 1 m2 (PV13369,  $2.00 \times 2.35$ )

### Description

**P4.** The anteroloph is lower than the other lophi. The paracone and the metacone are large and evident. The protoloph and the metaloph are directed anteriorly. The protoloph carries a large protoconule. The metaloph is not complete. The mesostyl is isolated from the paracone and the metacone.

**M1/2.** The anteroloph is well developed and it is not connected to the paracone. The protocone is well developed. The hypocone is weak, low, incorporated within the posteroloph and connected to the protocone. The posteroloph is connected to the metacone. The protoloph and the metaloph are parallel to each other and connected to the protocone. The mesostyl is present and isolated from the paracone and the metacone. The roots are not preserved.

**d4.** The anteroconulid is very small and it is placed anteriorly to the metaconid and the protoconid. The metaconid, the protoconid and the hypoconid are rounded. The metaconid is the highest cusp. The protoconid and the metaconid are connected by a low metalophid. The entoconid is smaller than the

other cusps, but distinct and connected to the posterolophid. The mesolophid is weak and separated from the entoconid. The mesoconid is absent.

**m2.** The anterolophid is weak and situated labially. It joins the metaconid to the protoconid. The metaconid is the highest cusp. The protoconid, the metaconid and the hypoconid are robust, while the entoconid is small but clearly distinct. It is connected to the posterolophid. The metalophid is weak and connected to the protoconid. The mesoconid is large, lower than the protoconid and the hypoconid. It is separated from these conids by two lingual furrows. The mesolophid is separated from the metaconid and the entoconid. The surface of the central valley is smooth. The molar has four roots, but one extra protrusion is present which may represent a fifth root.

### Remarks

*Palaeosciurus* is represented in Anatolia by several taxa. These are: *Palaeosciurus* cf. *feignouxi* from Kargı 2, *Palaeosciurus feignouxi* from Gökler, Kılçak 0, Kılçak 0<sup>n</sup>, Kılçak 3a and Kılçak 3b, *Palaeosciurus fissurae* from Sabuncubeli and Bornova, *Palaeosciurus* aff. *feignouxi* from Keseköy, *Palaeosciurus* indet. from Gördes and *Palaeosciurus* cf. *sutteri* from Kaplangı (De Bruijn et al. 2006; Bilgin et al. 2019; Bosma et al. 2019; Pelaez-Campomanes et al. 2019).

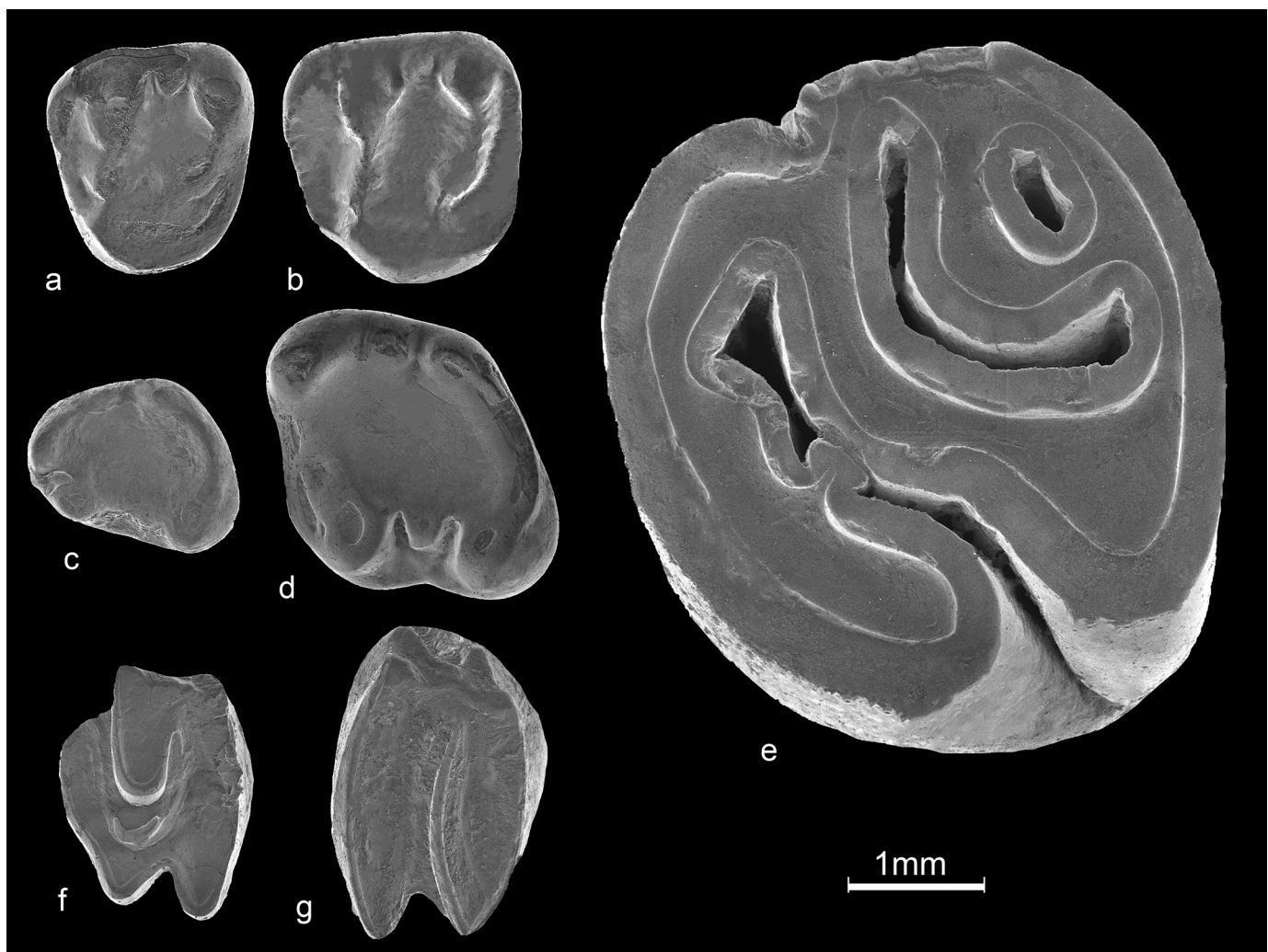


**Figure 10.** *Palaeosciurus fissurae* (A) P4 sin (PV13367), (B) M1/2 sin (PV13366), (C) d4 sin (PV13368), (D) m2 sin (PV13369); *Steneofiber eseri* (E) P4 sin (PV13672); Ochotonidae indet. (F) P3 sin (PV13673), (G) M2? sin (PV13674).

*Palaeosciurus* from Beydere 3 falls metrically within the range of *P. feignouxii* from the Kılçak section described by Bosma et al. (2019). However, the morphology of *Palaeosciurus* from Beydere 3 is different from *P. feignouxii*. The Beydere 3 assemblage does not show a strong anterolophid and metalophid in m2 and has an isolated mesostyle in M1/2. *Palaeosciurus* from Beydere 3 is morphologically compatible with *P. fissurae* from its type locality Wintershof-West described by Dehm (1950) and from Sabuncubeli and Bornova (De Bruijn et al. 2006; Bilgin et al. 2019). The Beydere 3 specimens are somewhat smaller than those from Bornova and Wintershof-West and within the range of the Sabuncubeli specimens. Apart from their smaller size, the morphology of Beydere 3 specimens fits well with the type population of *P. fissurae*.

Family Castoridae Hemprich 1820

Genus *Steneofiber* Geoffroy 1833

*Steneofiber eseri* (von Meyer 1846)

Figure 10 E

**Material and measurement.** 1 P4 (PV13672, 5.25 × 5.4)

### Description

**P4.** The tooth is worn. The outline of the molar is sub-rounded. The mesoflexus is closed and it is convexly curved from the labial border to the posterior side of the molar. The hypoflexus is directed anteriorly and ends adjacent to the parafossette. The constriction between the hypoflexus and parafossette is weak. The hypostria reaches less than half of the tooth height. The mesostria is very short (less than one third of the tooth height) and placed slightly anteriorly to enclosed mesoflexus. The metafossette is small and oval. The parafossette is larger than the metafossette. The roots are not preserved.

### Remarks

Beavers are not abundant in the early Miocene Anatolian assemblages. The family is represented by one species, *Steneofiber eseri*, which is known from Harami 4, Harami 5, Sabuncubeli and Kınık 2 (De Bruijn et al. 2006; Joniak et al. 2019). The *Steneofiber* specimen from Beydere 3 is morphologically similar to *S. eseri* from Ulm-Westtangente and Sabuncubeli (Stefen 1997; De Bruijn et al. 2006). The size is, however, larger than the Sabuncubeli specimens and within the lower dimensions of *S. eseri* from Ulm-Westtangente. Overall, we do not see any problem to attribute these specimens under *Steneofiber eseri*.

Order Lagomorpha Brandt 1855

Family Ochotonidae Thomas 1897

Ochotonidae indet.

Figure 10 F–G

**Material and measurement.** 1 P3 (PV13673, 1.35 × -), 1 M2 (PV13674, 1.42 × 2.18)

### Description

**P3.** The labial side of the P3 is broken. The protoloph is well developed. The hypoflexus separates the protocone and the hypocone. The hypocone is larger than the protocone. The paraflexus shows deep lingual convexity.

**M2.** The protocone and the hypocone of M2 are sharp and prominent. The metastyl is longer than the paracone.

### Remarks

Ochotonidae are represented by two species in the early Miocene of Anatolia: *Albertona balcanica* López Martínez 1986 from Çapak and *Albertona aegeensis*; Ünay and Göktaş 1999 from Söke and Dededağ (Ünay and Göktaş 1999; Bilgin et al. 2021). The presence of an ochotonid in Beydere 3 is important to show the full diversity of the fauna. Unfortunately, with the limited material available, we cannot make a closer identification.

### Discussion

#### The composition of the assemblage and the palaeoenvironmental considerations

The assemblage of Beydere 3 consists of 306 molars. However, the composition was calculated only on the basis of the 231 molars collected in the first campaign season (Table 6). Because the coarse material was lost in the second collecting season and only the fine material was processed, we could not use this material for assessing the composition of the assemblage.

The fauna consists of twelve rodent species belonging to four different families. As is the case for similarly aged assemblages, murids are the most dominant group in Beydere 3 (88.8% of all specimens and 89.2% of M1 + M2 + m1 + m2) (Table 6). They are represented by eight species belonging to six genera: *Eumyarion*, *Mirrabella*, *Cricetodon*, *Democricetodon*, *Megacricetodon* and *Vallaris*. The fauna is strongly dominated by *Eumyarion*. The latter genus is represented by three species: *Eumyarion* sp., *Eumyarion beyderensis* sp. nov. and *Eumyarion aegeaniensis* sp. nov. with about 48.3% of the assemblage, the most dominant species being *Eumyarion aegeaniensis*, comprising 32.7% of the assemblage. It is followed by *Megacricetodon hellenicus*, represented by 16.2%. In that respect, Beydere 3 is the locality that shows the first common occurrence of *Megacricetodon* in Anatolia. *Democricetodon doukasi* is the third most abundant species in the assemblage with about 13.8%. The large species *Cricetodon kasapligili*, *Mirrabella crenulata* and the small species *Vallaris zappai* are rare in the fauna and represented by 1.7%, 3.7% and 3.5%, respectively. Gliridae is the second most dominant family in the assemblage by 9.1%. The family is mostly represented by *Glirulus ekremi* with about 7.8% and only three specimens from *Glis* sp. comprise about 1.3% of the assemblage. Castoridae and Sciuridae are represented by one species only and are very limited: *Steneofiber eseri* with about 0.4% and *Palaeosciurus fissurae* with about 1.7%. In addition to the rodents, two ochotonid molars are also found.

Among the early Miocene rodent assemblages of Anatolia, Beydere 3 stands out by having *Eumyarion* and *Megacricetodon* species together in highest proportions. In other *Eumyarion*

**Table 6.** The rodent composition of Beydere 3 assemblage.

Rodent species	Total		M1+ M2+ m1+ m2		MNI	
	N	%	N	%	N	%
<i>Cricetodon kasapligili</i>	4	1.7	2	1.2	2	3.1
<i>Mirrabella crenulata</i>	9	3.9	4	2.5	4	6.3
<i>Eumyarion beyderensis</i> sp.nov.	25	10.8	19	11.8	8	12.3
<i>Eumyarion aegeaniensis</i> sp. nov.	76	32.7	59	36.6	20	31.2
<i>Eumyarion</i> sp.	11	4.8	7	4.4	2	3.1
<i>Megacricetodon hellenicus</i>	37	16.2	22	13.7	8	12.3
<i>Democricetodon doukasi</i>	35	15.2	24	14.9	7	11.1
<i>Vallaris zappai</i>	8	3.5	7	4.4	5	7.9
<i>Glis</i> sp.	3	1.3	2	1.2	1	1.6
<i>Glirulus ekremi</i>	18	7.8	12	7.5	5	7.9
<i>Palaeosciurus fissurae</i>	4	1.7	2	1.2	1	1.6
<i>Steneofiber eseri</i>	1	0.4	1(0)	0.6	1	1.6
<b>Σ</b>	<b>231</b>	<b>100</b>	<b>161</b>	<b>100</b>	<b>64</b>	<b>100</b>

dominated assemblages of the region, *Megacricetodon* is absent or represented by a few elements only. The species belonging to *Eumyarion* are considered wet and humid environment indicators (e.g., Pelaez-Campomanes et al. 2019). In that respect, Beydere 3 represents a similar habitat as Sabuncubeli and Keseköy. Beydere 3 is the youngest Anatolian fauna dominated by *Eumyarion* and the oldest fauna with a common occurrence of *Megacricetodon*. This intersection may be the only period in which these genera appear in equal numbers. In the following time period, we observe a sharp decrease in the number of *Eumyarion* specimens and an increase in the number of *Megacricetodon* specimens, which could be indicative of a change to drier environmental conditions as, for instance, suggested by the Çapak assemblage (Bilgin et al. 2021). Except for the dominance of the *Megacricetodon* and the presence of the different species of *Eumyarion*, Beydere 3 shares taxa with either Sabuncubeli and Keseköy or both (Table 7). Although of similar age, Beydere 3 may represent the first signal of an environmental change, but still represents relatively wet conditions, as also indicated by the presence of a beaver.

### The age of the assemblage

The assemblage of Beydere 3 shares the taxa *Cricetodon kasapligili*, *Vallaris zappai*, *Democricetodon doukasi*, *Glirulus ekremi* with the similarly aged assemblages Keseköy and Sabuncubeli. *Steneofiber eseri* and *Palaeosciurus fissurae* are also known from Sabuncubeli, whereas *Mirrabella crenulate* was described from Keseköy (Table 7). All these localities host a community predominantly consisting of *Eumyarion*. While Keseköy and Sabuncubeli contain *Eumyarion montanus* and *Eumyarion intercentralis*, Sabuncubeli also contains *Eumyarion orhani*. Beydere 3 yielded two new species of *Eumyarion*. *Eumyarion aegeaniensis* n. sp. from Beydere 3 shows characters more advanced than *E. orhani* from Sabuncubeli and more primitive than *E. bifidus* from Sandelzhausen. Thus, *Eumyarion aegeaniensis* n. sp. represents an intermediate morphology. On the other hand, while the *Mirrabella*

**Table 7.** Species list of rodents from the local zone D (MN3) localities of Anatolia. Data after De Bruijn and Saraç 1991; De Bruijn et al. 1993; De Bruijn and von Koenigswald 1994; Ünay 1994; Theocharopoulos 2000; Wessels et al. 2001; López-Antoñanzas et al. 2004; De Bruijn et al. 2006.

Species	Sabuncubeli	Keseköy	Beydere 3
<i>Cricetodon kasapligili</i>	x	x	x
<i>Democricetodon doukasi</i>	x	x	x
<i>Eumyarion montanus</i>	x	x	
<i>Eumyarion orhani</i>	x		
<i>Eumyarion intercentralis</i>	x	x	
<i>Eumyarion</i> sp.			x
<i>Eumyarion beyderensis</i>			x
<i>Eumyarion aegeaniensis</i>			x
<i>Enginia djanpolati</i>		x	
<i>Enginia gertcheki</i>		x	
<i>Mirrabella anatolica/crenulate</i>	x		
<i>Mirrabella crenulate</i>		x	x
<i>Megacricetodon</i> sp.		x	
<i>Megacricetodon hellenicus</i>			x
<i>Vallaris zappai</i>	x	x	x
<i>Debruijnina arpati</i>	x	x	
<i>Palaeosciurus feignouxii</i>		aff.	
<i>Palaeosciurus fissurae</i>	x		x
<i>Steneofiber eseri</i>	x		x
<i>Sayimys giganteus</i>		x	
<i>Glirulus ekremi</i>	x	x	x
<i>Glis galitopolui</i>	x	x	
<i>Glis</i> sp.			x
<i>Glirudinus engesseri</i>	aff.		
<i>Myomimus</i> sp.		x	

species from Sabuncubeli shows intermediate characters between *M. anatolica* and *M. crenulate*, Keseköy and Beydere 3 both yielded *M. crenulate*, whereas Aliveri and Karydia both yielded *M. tuberosa*. The presence of *Megacricetodon hellenicus* and *Mirrabella crenulate* together may indicate that Beydere 3 represents the first occurrence of *M. hellenicus* and should be older than Aliveri and Karydia.

The advanced characters of *Eumyarion aegeaniensis* n. sp. and the presence of *M. crenulate* indicate that Beydere 3 assemblage is younger than Sabuncubeli and older than Aliveri. Based on the presence of *M. crenulate*, *Cricetodon kasapligili*, *Democricetodon doukasi* and *Megacricetodon*, it should be placed in local zone D, which is correlated with MN3 (Ünay et al. 2003). Radiometric dating of ashes overlying the section indicates the age of the locality is older than 18.21 ( $\pm$  0.19) Ma. Although Keseköy and Beydere 3 share many common species, there are no clear evolutionary differences between the assemblages from these localities. Therefore, it is not possible to propose a precise relative temporal position between Keseköy and Beydere 3.

### Conclusion

The Beydere 3 assemblage comprises twelve rodent and a lagomorph taxa; the murids *Cricetodon kasapligili*, *Mirrabella crenulate*, *Eumyarion beyderensis* n. sp., *E. aegeaniensis* n. sp., *Eumyarion* sp., *Megacricetodon hellenicus*, *Democricetodon doukasi* and *Vallaris zappai*, the glirids *Glirulus ekremi*, *Glis* sp., the sciurid *Palaeosciurus fissurae*, the beaver *Steneofiber eseri* and the lagomorph Ochotonidae indet. Based on the radiometric dating, the locality is older than 18.21 ( $\pm$  0.19) Ma. The fauna presents the familiar composition of the other assemblages of Anatolian local zone D, like Sabuncubeli and Keseköy. The most significant feature of this time interval is the dominance and diversity of the murid *Eumyarion*. In contrast to the Sabuncubeli and Keseköy, Beydere 3 has two *Eumyarion* species of similar lower dentition and size. In addition, Beydere 3 stand out in harbouring the first common occurrence of *Megacricetodon*. It is the only known fauna that shows an equal proportion of *Eumyarion* and *Megacricetodon*. The following time period shows a serious decrease in number of *Eumyarion* specimens and an increase in numbers of *Megacricetodon* specimens. The dominance of the *Eumyarion* in the assemblage indicates a swampy palaeoenvironment confirmed by the presence of a beaver in the locality.

### Acknowledgments

The staff of the Natural History Museum of Ege University made us feel at home during our campaigns and we are grateful for all their support. Aytekin Tan, Kazım Halaçlar, Rutger van den Hoek Ostende, Panagiotis Skandalos, Mark Doeland and Yanell Braumüller helped us during the field-work campaign and their work and warm companionship are gratefully acknowledged. We dedicate this paper to Hans de Bruijn, who recently passed away. His work was a great inspiration for many of us.

We are indebted to Şevket Şen, Vicente D. Crespo and Jerome Prieto, as well as the anonymous reviewer for their valuable comments, which have improved the manuscript.

### Disclosure statement

No potential conflict of interest was reported by the author(s).

### Funding

This work was supported by the Ege Üniversitesi (TTM/001/2016,TTM/002/2016);National Geographic Society (GEFNE 140-15); Spanish Ministry of Science and Innovation (PGC2018-094122-B-I00); Univerzita Komenského v Bratislave (UK/400/2021); Vedecká Grantová Agentúra MŠVVaŠ SR a SAV (1/0164/19, 1/0533/21) and Slovak Research and Development Agency under contracts (APVV-15-0575).



## ORCID

Melike Bilgin  <http://orcid.org/0000-0003-4047-2865>  
 Peter Joniak  <http://orcid.org/0000-0002-0244-951X>  
 Pablo Peláez Campomanes  <http://orcid.org/0000-0002-6551-1026>  
 Fikret Göktaş  <http://orcid.org/0000-0002-0011-4361>  
 Serdar Mayda  <http://orcid.org/0000-0001-5432-3559>  
 Lars W. van den Hoek Ostende  <http://orcid.org/0000-0003-3114-0121>

## References

- Akyürek B, Soysal Y. 1981. Main geological features of the area South of Biga Peninsula (Savaştepe-Kırkağaç-Bergama-Ayvalık). *Bull Mineral Res Explor.* 95(96):1–12.
- Bilgin M, Joniak P, Mayda S, Göktaş F, Kaya T, Peláez-Campomanes P, Van den Hoek Ostende LW. 2019. Sabuncubeli too, Bornova, a second micromammal assemblage from the Sabuncubeli section (early Miocene, western Anatolia). In: Van den Hoek Ostende LW, Mayda S, and Kaya T, editors. Taking the Orient Express? The role of Anatolia in Mediterranean Neogene palaeobiogeography. *Palaeobiodiver Palaeoenvir.* 99:655–671. doi:10.1007/s12549-019-00395-2.
- Bilgin M, Joniak P, Mayda S, Göktaş F, Peláez-Campomanes P, Van den Hoek Ostende LW. 2021. Micromammals from the late early Miocene of Çapak (western Anatolia) herald a time of change. *J Paleontol.* 1–18. doi:10.1017/jpa.2021.27.
- Bosma AA, de Bruijn H, Wessels W. 2019. Early and middle Miocene Scuriidae (Mammalia, Rodentia) from Anatolia, Turkey. *J Vertebr Paleontol.* 38(6). doi:10.1080/02724634.2018.1537281.
- Brinkmann R. 1966. Geotektonische Gliederung von Westanatolien [Geotectonic guidance of West Anatolia]. *Neues Jahrb Geol Palaontol-Monatsh.* 10:603–618.
- Çınar N. 2011. Doğu Akdeniz Bölgesinin Erken Miyosen Yaşlı Cricetodontinleri [Early Miocene Cricetodontini from eastern Anatolia] [master's thesis]. Ankara University, Institute of Natural Sciences, Department of Geology. 199 p.
- Cuenca-Bescós G. 1988. Revisión de los Scuriidae del Aragoniense y del Ramblense en la fosa de Calatayud-Montalbán [Revision of the Aragonian and Ramblense Scuriidae in the Calatayud-Montalbán]. *Scr Geol.* 87:1–127.
- Daams R, Freudenthal M. 1988a. Synopsis of the Dutch Spanish collaboration program in the Aragonian type area. 1975–1986. *Scr Geol Special Issue.* 1:3–18.
- Daams R, Freudenthal M. 1988b. Cricetidae (Rodentia) from the type-Aragonian; the genus *Megacricetodon*. *Scr Geol Special Issue.* 1:39–132.
- Daxner-Höck G. 1998. Wirbeltiere aus dem Unter-Miozän des Lignit-Tagebaues Oberdorf (Weststeirisches Becken, Österreich) 7. Rodentia 2 und Lagomorpha (Mammalia). [Vertebrates from the Lower Miocene of the Oberdorf lignite mine (Weststeirisches Basin, Austria) 7. Rodentia 2 and Lagomorpha (Mammalia)]. *Ann Naturhist Mus Wien.* 99:139–162.
- De Bruijn H, Saraç G. 1991. Early Miocene rodent faunas from the eastern Mediterranean area. Part I. The genus *Eumyarion*. *Proc K NedAkad Wet.* 94(1):1–36.
- De Bruijn H, Saraç G. 1992. Early Miocene rodent faunas from the eastern Mediterranean area. II: *mirabella* (Paracricetodontina, Muroidea). *Proc K NedAkad WetSer B.* 95(1):25–40.
- De Bruijn H, Fahlbusch V, Saraç G, Ünay E. 1993. Early Miocene rodent faunas from the eastern Mediterranean area .3. The genera *Deperetomys* and *Cricetodon* with a discussion of the evolutionary history of the Cricetodontini. *Proc K NedAkad WetSer B.* 96(2):151–216.
- De Bruijn H, von Koenigswald W. 1994. Early Miocene faunas from the eastern Mediterranean area. Part V. The genus *Enginia* (Muroidea) with a discussion of the incisor enamel. *Proc K AkadWet.* 97(4):381–405.
- De Bruijn H. 1998. Vertebrates from the Early Miocene lignite deposits of the opencast mine Oberdorf (Western Styrian Basin, Austria): 6. Rodentia 1 (Mammalia). *Ann Naturhist Mus Wien.* 99(A):99–137.
- De Bruijn H, Van den Hoek Ostende L, Kristkoiz-Boon MR, Theocharapoulos K, Ünay E. 2003. Rodents, lagomorphs and insectivores, from the middle Miocene hominoid locality of Çandır (Turkey). *Courier Forschungsinstitut Senckenberg.* 240:51–87.
- De Bruijn H, Mayda S, Van den Hoek Ostende LW, Kaya T, Saraç G. 2006. Small mammals from the Early Miocene of Sabuncubeli (Manisa, S.W. Anatolia, Turkey). *Beiträge Paläontologie.* 30:57–87.
- De Bruijn H. 2009. The *Eumyarion* (Mammalia, Rodentia, Muridae) assemblage from Sandelzhausen (Miocene, Southern Germany): a test on homogeneity. *Paläontol Z.* 83:77–83. doi:10.1007/s12542-009-0001-0.
- De Bruijn H, Markovic Z, Wessels W. 2013. Late Oligocene rodents from Banovići. *Palaeodiversity.* 6:63–105.
- Dehm R. 1950. Die Nagetiere aus dem Mittel-Miozän (Burdigalium) von Wintershof-West bei Eichstätt in Bayern [The rodents from the Middle Miocene (Burdigalium) of Wintershof-West near Eichstätt in Bavaria]. *Neues Jahrb Mineral Geol Paläontol.* 91(B):321–428.
- Dinçarslan I, Suata-Alpaslan F. 2016. Hafik-Düzyayla (Sivas Kd) Yöresinin Stratigrafisi ve Küçük Memeli Fosillerinin Taksonomik Biyokronolojik ve Paleobiyoğrafik İncelemesi [Stratigraphy of Hafik-Düzyayla Region and Taxonomic, Biocronological and Paleobiogeographical Study of Small Mammal Fossils]. *Cumhuriyet Üniversitesi Fen-Edebiyat Fakültesi Fen Bilimleri Dergisi.* 37(3):248–270. doi:10.17776/csj.82281.
- Durgut NÇ, Engin Ü. 2016. Cricetodontini from the early Miocene of Anatolia. *Bull Mineral Res Explor.* 152:85–119.
- Fahlbusch V. 1964. Die Cricetiden (Mammalia) der Oberen Süßwasser-Molasse Bayern [The Cricetidae (Mammalia) of the Upper Freshwater Molasse Bavaria]. *Abh BayerAkad WissMath-naturwiss.* 118:1–135.
- García-Paredes I, Peláez-Campomanes P, Alvarez-Sierra MA. 2010. *Microdromys remmertii* sp. nov., a new Gliridae (Rodentia, Mammalia) from the Aragonian type area (Miocene, Calatayud Montalbán Basin, Spain). *J Vertebr Paleontol.* 30:1594–1609. doi:10.1080/02724634.2010.501453.
- Hartenberger JL. 1965. Les Cricetidae (Rodentia) de Can Llobateres (Néogène d'Espagne) [The Cricetidae (Rodentia) from Can Llobateres (Neogene of Spain)]. *Bull Soc Géol France.* 7:487–498. doi:10.2113/gssgfbull.S7-VII.3.487.
- Heller F. 1936. Eine oberpliozäne Wirbeltierfauna aus Rheinhessen [A Upper Pliocene vertebrate fauna from Rheinhessen]. *Neues Jahrb MineralGeol PaläontolAbt B Beil Bd.* 76:99–160.
- Huguene M, Mein P. 1965. Lagomorphes et rongeurs du Neogene de Lissieu (Rhône) [Lagomorphs and rodents from the Neogene of Lissieu (Rhône)]. *Doc Lab Geol Faculte Sci Lyon.* 12:109–123.
- Huguene M. 1999. Family Castoridae. In: Rössner GE, Heissig K, editors. The Miocene land Mammals of Europe. München: Friedrich Pfeil; p. 281–300.
- Joniak P, Peláez-Campomanes P, Van den Hoek Ostende LW, Rojay B. 2017. Early Miocene rodents of Gökler (Kazan Basin, Central Anatolia, Turkey). *Hist Biol.* 31(8):982–1007. doi:10.1080/08912963.2017.1414211.
- Joniak P, Peláez-Campomanes P, Mayda S, Bilgin M, Halaçlar K, Van den Hoek Ostende LW. 2019. New faunas of small mammals from old Harami mine (early Miocene, Anatolia, Turkey). In: Van den Hoek Ostende L W, Mayda S, and Kaya T, editors. Taking the Orient Express? The role of Anatolia in Mediterranean Neogene palaeobiogeography. *Palaeobiodiver Palaeoenvir.* 99:673–700. doi:10.1007/s12549-018-0349-9.
- Kaya O, Ünay E, Göktaş F, Saraç G. 2007. Early Miocene stratigraphy of central west Anatolia, Turkey: implications for the tectonic evolution of the eastern Aegean area. *Geol J.* 42:85–109. doi:10.1002/gj.1071.
- Klein Hofmeijer G, de Bruijn H. 1988. The mammals from the lower Miocene of Aliveri (Island of Evia, Greece). *Proc K Ned Akad Wet Ser B.* 91:185–204.
- Koppers AAP. 2002. ArArCALC-software for 40Ar/39Ar agecalculations. *Comput Geosci.* 28:605–619. doi:10.1016/S0098-3004(01)00095-4.
- Kuiper KF, Deino A, Hilgen FJ, Krijgsman W, Renne PR, Wijbrans JR. 2008. Synchronizing rock clocks of Earth history. *Science.* 320:500–504. doi:10.1126/science.1154339.
- Lartet E. 1851. Notice sur la colline de Sansan, suivie d'une récapitulation des diverses espèces d'animaux vertébrés fossiles trouvés soit à Sansan, soit dans d'autres gisements du terrain tertiaire Miocène dans le bassin Sous-Pyrénéen, avec une liste des coquilles terrestres, lacustres et fluviales fossiles du même terrain [Note on the Hill of Sansan, followed by a recapitulation of the diverse vertebrate fossils found at Sansan and other localities from the Miocene deposit of the Sub-Pyrenean Basin, with a list of terrestrial, lacustrine and fluvial fossil shells from this deposit]. *Auch (France): J. A. Portes;* p. 47.
- López Martínez N. 1986. The mammals from the lower Miocene of Aliveri (Island of Evia, Greece). VI. The ochotonid lagomorph *Albertona balkanika* n. gen. n. sp. and its relationships. *Proc K Ned Akad Wet Ser B.* 89:177–194.
- López-Antoñanzas R, Sen S, Saraç G. 2004. A new large ctenodactylid species from the lower Miocene of Turkey. *J Vertebr Paleontol.* 24(3):676–688. doi:10.1671/0272-4634(2004)024[0676:ANLCSF]2.0.CO;2
- Mayr H. 1979. Gebiss morphologische Untersuchungen an miozänen Gliriden (Mammalia, Rodentia) Süddeutschlands [Dental morphological investigations on Miocene glirids (Mammalia, Rodentia) from southern Germany] [dissertation]. University Munich.
- Oliver A, Peláez-Campomanes P. 2013. *Megacricetodon vandermeuleni*, sp. nov. (Rodentia, Mammalia), from the Spanish Miocene: a new evolutionary framework for *Megacricetodon*. *J Vertebr Paleontol.* 33:943–955. doi:10.1080/02724634.2013.743896.

- Oliver A, Peláez-Campomanes P. 2014. Evolutionary patterns of early and middle Aragonian (Miocene) of *Megacricetodon* (Rodentia, Mammalia) from Spain. *PalaeontographicaA*. 303:85–135. doi:10.1127/pala/303/2014/85.
- Peláez-Campomanes P, Göktaş F, Kaya T, Joniak P, Bilgin M, Mayda S, Van den Hoek Ostende LW. 2019. Gördes, a new early Miocene micromammal assemblage from western Anatolia. In: Van den Hoek Ostende L W, Mayda S, and Kaya T, editors. Taking the Orient Express? The role of Anatolia in Mediterranean Neogene palaeobiogeography. *Palaeobiodiver Palaeoenvir*. 99:639–653. doi:10.1007/s12549-018-0346-z.
- Prieto J, Rummel M. 2016. Some considerations about the small mammal evolution in South Germany, with emphasis on late Burdigalian earliest Tortonian (Miocene) cricetid rodents. *Comptes Rendus*. 15(7):837–854.
- Saraç G. 2003. Türkiye Omurgalı Fossil Yatakları Rapor Yazısı [Report of Mammalian Fossils Localities in Turkey]. Maden Tetkik Arama Genel Müdürlüğü (Mineral Res Explor Inst (MTA) Turkey Rep). 10609:218.
- Schaub S, Zapfe H. 1953. Die Fauna der Miozänen Spaltenfüllung von Neudorf an der March, Simplicidentata [The fauna of the Miocene fissures from Neudorf an der March, Simplicidentata]. *Sitzber ÖsterreichAkad WissMath Naturwisse Kl Abt 1*. 162(3):181–215.
- Schinz HR. 1845. Systematisches verzeichniss aller bis jetzt bekannten Säugethiere, oder, Synopsis mammalium, nach dem Cuvier'schen system. Vol. 2, 1845-46. Solothurn: Jent und Gassmann.
- Schneider B, Kuiper KF, Postma O, Wijbrans J. 2009. 40Ar/39Ar geochronology using a quadrupole mass spectrometer. *Quat Geochronol*. 4(6):508–516. doi:10.1016/j.quageo.2009.08.003.
- Stefen C. 1997. *Steneofiber eseri* (Castoridae, Mammalia) von der Westtangente bei Ulm im Vergleich zu anderen Biberpopulationen [*Steneofiber eseri* (Castoridae, Mammalia) from the Westtangente near Ulmin with other beaver assemblages]. *Stutt BeitrNaturk Ser B (Geol Paläont)*. 255:1–73.
- Steiger RH, Jager E. 1977. Subcommission on geochronology; Convention on the use of decay constants in geo- and cosmochronology. *Earth Planet Sci Lett*. 36:359–362. doi:10.1016/0012-821X(77)90060-7.
- Taylor JR. 1997. An Introduction to Error Analysis: the Study of Uncertainties in Physical Measurements. 2nd ed. Sausalito (CA): University Science Books; p. 327.
- Theocharopoulos C. 2000. Late Oligocene - middle Miocene *Democricetodon*, *Spanocricetodon* and *Karydomys* n. gen. from the eastern Mediterranean area. *Gaia*. 8:1–92.
- Ünay E. 1994. Early Miocene rodent faunas from the eastern Mediterranean area. Part IV. The Gliridae. *Proc K NedAkad WetSer B*. 97:445–490.
- Ünay E, Göktaş F. 1999. Late early Miocene and Quaternary small mammals in the surroundings of Söke (Aydın): preliminary results. *Geol Bull Turkey*. 42:99–113.
- Ünay E, Göktaş F. 2000. Small mammal biochronology of the early Miocene lignitiferous sediments around Kınık (Gördes): preliminary results. *Geol Bull Turkey*. 43:1–5.
- Ünay E, De Bruijn H, Saraç G. 2003. A preliminary zonation of the continental Neogene of Anatolia based on rodents. *Deinsea*. 10, 539–547.
- Van den Hoek Ostende LW. 1992. Insectivore faunas from the lower Miocene of Anatolia. part 1. Erinaceidae. *Proc K NedAkad WetSer B*. 95(4):437–467.
- Van den Hoek Ostende LW. 1995a. Insectivore faunas from the Lower Miocene of Anatolia. Part 2: *dinosorex* (Heterosoricidae). *Proc K Ned Akad WetSer B*. 98(1):1–19.
- Van den Hoek Ostende LW. 1995b. Insectivore faunas from the Lower Miocene of Anatolia. Part 3: dimylidae. *Proc K NedAkad WetSer B*. 98(1):19–38.
- Van den Hoek Ostende LW. 1997. Insectivores from the Lower Miocene of Anatolia. part 4: the genus *Desmanodon* (Talpidae) with the description of a new species from the Lower Miocene of Spain. *Proc K NedAkad Wet*. 100(1–2):27–65.
- Van den Hoek Ostende LW. 2001. Insectivore faunas from the Lower Miocene of Anatolia. Part 8: stratigraphy, palaeoecology, palaeobiogeography. *Scr Geol*. 122:101–122.
- Vasileiadou K, Koufos GD. 2005. The micromammals from the Early/Middle Miocene locality of Antonios, Chalkidiki, Greece. *Ann Paleontol*. 91(3):197–225. doi:10.1016/j.annpal.2005.06.002.
- Wessels W, Theocharopoulos KD, De Bruijn H, Ünay E. 2001. Myocricetodontinae and Megacricetodontini from the lower Miocene of NW Anatolia. *Lynx*. 32:371–388.
- Wijbrans JR, Pringle MS, Koppers AAP, Scheveers R. 1995. Argon geochronology of small samples using the Vulkan argon laser probe. *Proc K NedAkad Wet*. 9(2):185–218.
- Wijbrans J, Németh K, Martin U, Balogh K. 2007. 40Ar/39Ar Geochronology of Neogene phreatomagmatic volcanism in the Western Pannonian Basin, Hungary. *J Volcanol Geotherm Res*. 164:193–204. doi:10.1016/j.jvolgeores.2007.05.009.
- Wu W. 1993. Neue Gliridae (Rodentia, Mammalia) aus untermiozänen (Orleanischen) Spaltenfüllungen Süddeutschlands. *Documenta Naturae*. 81:1–149.